Electronic Supplementary Material (ESI) for New Journal of Chemistry.

Electronic Supplementary Information

A series of trinuclear zinc(II) complexes with reduced Schiff base ligands: Turn-off fluorescent chemosensors with high selectivity for nitroaromatics

Mainak Karmakar, Sourav Roy and Shouvik Chattopadhyay*

Department of Chemistry, Inorganic Section, Jadavpur University, Kolkata - 700032, India.

E-mail: shouvik.chem@gmail.com

Experimental Section

Materials

All chemicals were of reagent grade and used as purchased from Sigma-Aldrich without further purification.

Caution!!! Although no problems were encountered in this work, organic ligands in the presence of azide are potentially explosive. Only a small amount of the material should be prepared and it should be handled with care.

Preparation

Preparation of the ligand, 2,2'-[(1,3-propanediyl)bis(iminomethylene)]bis[6-ethoxyphenol] (H_2L^1)

A Schiff base ligand, $H_2L^{1`}$ {$H_2L^{1'}$= *N,N'-bis(3-ethoxysalicylidene)propane-1,3-diamine*}, was synthesized by refluxing 1,3-diaminopropane (2 mmol, 0.21 mL) with 3-

ethoxysalicylaldehyde (4 mmol, 0.660 g) in methanol (20 mL) solution for ca. 2h. The solution (20 mL) was then cooled to 0°C and solid sodium borohydride (6 mmol, 0.225 g) was added to it slowly with constant stirring. The resulting solution was acidified with glacial acetic acid (5 mL) and then evaporated to dryness under reduced pressure in a rotary evaporator (~60°C). The residue was then dissolved in water (15 mL) and extracted with dichloromethane (15 mL). The solvent i.e. dichloromethane was then evaporated under reduced pressure using a rotary evaporator to get the reduced Schiff base ligand, H_2L^1.

Preparation of the ligand, 2,2'-[(2,2-dimethyl-1,3-propanediyl)bis(iminomethylene)]bis[6-methoxyphenol] (H_2L^2)

Another Schiff base ligand, $H_2L^{2'}$ {$H_2L^{2'}$ = *N,N'-bis(3-methoxysalicylidene)-2,2-dimethylpropane-1,3-diamine*}, was synthesized by refluxing of 2,2-dimethyl-1,3-diaminopropane (2 mmol, 0.22 mL) with 3-methoxysalicylaldehyde (4 mmol, 0.610 g) in methanol (20 mL) solution for ca. 2h. It was then reduced in a similar method as that applied to prepare H_2L^2.

Preparation of the ligand, 2,2'-[(2,2-dimethyl-1,3-propanediyl)bis(iminomethylene)]bis[6-ethoxyphenol] (H_2L^3)

A Schiff base ligand, $H_2L^{3'}$ {$H_2L^{3'}$= *N,N'-bis(3-ethoxysalicylidene)2,2-dimethylpropane-1,3-diamine*}, was synthesized by refluxing of 2,2-dimethyl-1,3-propane diamine (2 mmol, 0.22 mL) with 3-ethoxysalicylaldehyde (4 mmol, 0.660 g) in methanol (20 mL) solution for ca. 2h. It was then reduced in a similar method as described above

Preparation of complexes

*$[\{(N_3)Zn(L^1)\}_2Zn]$ (**1**)*

A methanol solution of zinc(II) acetate dihydrate (3 mmol, 0.660 g) was added to the methanol solution of the ligand H_2L^1, with stirring. The stirring was continued for additional 2 h. An aqueous methanol (1:1) solution of sodium azide (2 mmol, 0.130 g) was then added to it and stirred further for ca. 2h. It was kept in open air at room temperature for 2 days. White crystalline product was collected by filtration. X-ray quality single crystals were collected from this crystalline product.

Yield: 0.697 g, 68% (based on zinc). Anal. Calc. for $C_{42}H_{56}N_{10}O_8Zn_3$ (1025.14): C, 49.21; H, 5.51; N, 13.66 %. Found: C, 49.1; H, 5.3; N, 13.8 %. FT-IR (KBr, cm^{-1}): 3247-3140 (ν_{N-H}); 2978-2847 (ν_{C-H}); 2053 (ν_{N3}). λ_{max} (nm) [ε_{max}(lit mol^{-1} cm^{-1})] (DMF): 290 (0.89 $\times 10^4$), 373 (80).

*$[\{(SCN)Zn(L^1)\}_2Zn]$ (**2**)*

Complex **2** was prepared in a similar method as that of complex **1**, except that sodium thiocyanate (2 mmol, 0.160 g) was used instead of sodium azide. The solution was kept in open air at room temperature for 2 days. White crystalline product was collected by filtration. X-ray quality single crystals were collected from this crystalline product.

Yield: 0.740 g, 70% (based on zinc). Anal. Calc. for $C_{44}H_{56}N_6O_8S_2Zn_3$ (1057.24): C, 49.99; H, 5.34; N, 7.95 %. Found: C, 49.8; H, 5.2; N, 8.1 %. FT-IR (KBr, cm^{-1}): 3247-3222 (ν_{N-H}); 2978-2855 (ν_{C-H}); 2032 (ν_{SCN}). λ_{max} (nm) [ε_{max}(lit mol^{-1} cm^{-1})] (DMF): 288 (1.35×10^4), 375 (70).

*[{(SCN)Zn(L^2)}$_2$Zn] (**3**)*

Complex **3** was prepared in a similar method as that of complex **2**, except that H_2L^2 was used instead of H_2L^1. The solution was kept in open air at room temperature for 2 days. White crystalline product was collected by filtration. X-ray quality single crystals were collected from this crystalline product.

Yield: 0.760 g, 72% (based on zinc). Anal. Calc. for $C_{44}H_{56}N_6O_8S_2Zn_3$ (1057.24): C, 49.99; H, 5.34; N, 7.95 %. Found: C, 49.7; H, 5.2; N, 8.1%. FT-IR (KBr, cm^{-1}): 3274-3180 ($\nu_{N–H}$); 2974-2888 ($\nu_{C–H}$); 2035 (ν_{SCN}). λ_{max} (nm) [ε_{max}(lit mol^{-1} cm^{-1})] (DMF): 288 (1.55x10^4), 373 (81).

*[{(N_3)Zn(L^2)}$_2$Zn] (**4**)*

Complex **4** was prepared in a similar method as that of complex **3**, except that sodium azide (2 mmol, 0.130 g) was used instead of sodium thiocyanate. The solution was kept in open air at room temperature for 2 days. White crystalline product was collected by filtration. X-ray quality single crystals were collected from this crystalline product.

Yield: 0.685 g, 67% (based on zinc). Anal. Calc. for $C_{42}H_{56}N_{10}O_8Zn_3$ (1025.14): C, 44.21; H, 5.51; N, 13.66 %. Found: C, 44.1; H, 5.3; N, 13.8 %. FT-IR (KBr, cm^{-1}): 3267-3162 ($\nu_{N–H}$); 2923-2831 ($\nu_{C–H}$); 2059 (ν_{N3}). λ_{max} (nm) [ε_{max} (lit mol^{-1} cm^{-1})] (DMF): 288 (1.54x10^4), 373 (102).

*[{(N_3)Zn(L^3)}$_2$Zn]·CH_2CL_2 (**5**)*

Complex **5** was prepared in a similar method as that of complex **4**, except that H_2L^3 was used instead of H_2L^2. It was kept in open air at room temperature for 2 days. White crystalline product was collected by filtration. X-ray quality single crystals were collected from this crystalline product.

Yield: 0.800 g, 69% (based on zinc). Anal. Calc. for $C_{46}H_{58}N_{10}O_8Zn_3$ (1160.12): C, 51.10; H, 5.97; N, 12.95 %. Found: C, 50.9; H, 5.8; N, 13.1 %. FT-IR (KBr, cm^{-1}): 3271-3164 (ν_{N-H}); 2967-2819 (ν_{C-H}); 2058 (ν_{N3}). λ_{max} (nm) [ε_{max}(lit mol^{-1} cm^{-1})] (DMF): 285 ($1.43x10^4$), 376 (72).

Physical measurements

Elemental analyses (carbon, hydrogen and nitrogen) were performed using a Perkin-Elmer 240C elemental analyzer. IR spectra in KBr (4500-500 cm^{-1}) were recorded with a Perkin-Elmer Spectrum Two spectrophotometer. Electronic spectra in DMF were recorded on a JASCO V-630 spectrophotometer. The steady-state fluorescence emission spectra were recorded using a Shimadzu RF-5301PC spectrofluorometer after proper background correction with individual solvents in quartz cells with 1 cm path length. Fluorescence lifetime measurements were recorded using Hamamatsu MCP photomultiplier (R3809) and were analyzed by using IBHDAS6 software. The emissions of complexes are tentatively attributed to the intra-ligand transitions modified by metal coordination. Intensity decay profiles were fitted to the sum of exponentials series $I(t)=\sum_i \alpha_i \exp\left({}^{-t}/_{\tau_i}\right)$, where α_i was a factor representing the fractional contribution to the time resolved decay of the component with a lifetime of τ_i. Bi-exponential function was used to fit the decay profile for both complexes, with obtaining χ^2 close to 1. The intensity-averaged life time (τ_{av}) was determined from the result of the exponential model using

$\tau_{av} = \frac{\sum_i \alpha_i \tau_i^2}{\sum_i \alpha_i \tau_i}$, where α_i and τ_i are the pre-exponential factors and excited state luminescence decay time associated with the *i*-th component, respectively. Electrospray ionization mass spectra were recorded using Waters QTOF Micro YA263. The powder XRD data were collected on a Bruker D8 Advance X-ray diffractometer using Cu K_α radiation (λ = 1.548 Å) generated at 40 kV and 40 mA. The PXRD spectra were recorded in a 2θ range of 5-50° using 1-D Lynxeye detector at ambient conditions.

X-ray Crystallography

Suitable single crystals of complexes **1**-**5** were used for data collection using a 'Bruker D8 QUEST area detector' diffractometer equipped with graphite-monochromated Mo K_α radiation (λ = 0.71073 Å). The molecular structures were solved by direct method and refined by full-matrix least squares on F^2 using the SHELX-18 package.[1] Non-hydrogen atoms were refined with anisotropic thermal parameters. The hydrogen atoms attached to nitrogen atoms were located by difference Fourier maps and were kept at fixed positions. All other hydrogen atoms were placed in their geometrically idealized positions and constrained to ride on their parent atoms. Multi-scan empirical absorption corrections were applied to the data using the program SADABS.[2] The crystal structure of complex **4** contains solvent accessible voids. PLATON/SQUEEZE has been employed to produce a set of void-free diffraction intensities. Details about the SQUEEZE procedure have been given in the CIF file.

Table S1: Selected bond lengths (Å) of complexes **1**-**5**.

Complex	**1**	**2**	**3**	**4**	**5**
Zn(1)-O(1)	2.070(3)	2.061(2)	2.066(3)	2.016(2)	2.021(2)
Zn(1)-O(2)	1.992(3)	2.010(2)	2.001(3)	2.053(2)	2.0548(19)
Zn(1)-N(1)	2.053(4)	2.082(3)	2.069(4)	2.160(3)	2.139(2)
Zn(1)-N(2)	2.151(5)	2.147(3)	2.165(4)	2.072(2)	2.085(3)
Zn(1)-N(5)	2.010(4)	-	2.013(4)	2.009(2)	2.011(3)
Zn(1)-N(3)	-	2.004(3)	-	-	-
Zn(2)-O(1)	2.025(3)	2.043(2)	2.038(3)	1.995(2)	1.995(2)
Zn(2)-O(2)	1.998(3)	1.982(2)	2.004(3)	2.039(2)	2.038(2)
Zn(2)-O(3)	-	-	-	2.346(1)	2.307(2)
Zn(2)-O(4)	2.379(4)	2.323(2)	2.300(3)	-	-
Zn(2)-O(5)	2.007(3)	-	2.018(3)	1.994(1)	2.003(2)
Zn(2)-O(1)[a]	-	2.043(2)	-	-	-
Zn(2)-O(6)	1.995(3)	-	2.005(3)	2.007(1)	2.028(2)
Zn(2)-O(2)[a]	-	1.982(2)	-	-	-
Zn(2)-O(8)	2.300(4)	-	2.345(3)	-	-
Zn(2)-O(7)	-	-	-	2.333(2)	2.333(3)
Zn(2)-O(4)[a]	-	2.323(2)	-	-	-
Zn(3)-O(5)	2.059(3)	-	2.054(3)	2.038(1)	2.032(2)
Zn(3)-O(6)	1.982(3)	-	2.047(3)	2.060(1)	2.055(2)

Zn(3)-N(3)	2.056(4)	-	2.099(4)	2.120(2)	2.149(3)
Zn(3)-N(4)	2.142(4)	-	2.139(4)	2.124(2)	2.092(3)
Zn(3)-N(6)	-	-	2.012(4)	-	-
Zn(3)-N(8)	1.995(4)	-	-	1.987(2)	2.005(3)

Symmetry transformations: [a] = 1-x,y,3/2-z

Table S2: Selected bond angles (°) for complexes **1**-**5**.

Complex	**1**	**2**	**3**	**4**	**5**
O(1)-Zn(1)-O(2)	77.04(11)	76.83(8)	76.06(10)	77.16(7)	76.30(8)
O(1)-Zn(1)-N(1)	91.79(14)	92.10(10)	92.23(11)	89.40(8)	88.01(10)
O(1)-Zn(1)-N(2)	164.23(12)	164.94(11)	161.86(12)	133.32(8)	132.36(10)
O(1)-Zn(1)-N(5)	97.95(14)	-	99.88(13)	115.27(9)	118.82(13)
O(1)-Zn(1)-N(3)	-	97.28(11)	-	-	-
O(2)-Zn(1)-N(1)	129.01(12)	131.03(10)	125.07(11)	163.84(7)	161.24(9)
O(2)-Zn(1)-N(2)	88.54(13)	89.30(11)	87.01(12)	92.27(8)	91.81(10)
O(2)-Zn(1)-N(5)	118.40(14)	-	116.39(14)	101.51(9)	102.60(11)
O(2)-Zn(1)-N(3)	-	114.33(10)	-	-	-
N(1)-Zn(1)-N(2)	92.41(16)	92.67(13)	92.24(12)	90.51(9)	91.27(12)
N(1)-Zn(1)-N(5)	112.34(15)	-	118.48(14)	92.26(10)	93.90(13)
N(1)-Zn(1)-N(3)	-	114.34(12)	-	-	-
N(2)-Zn(1)-N(5)	94.48(15)	-	93.38(15)	111.38(9)	108.75(13)

N(2)-Zn(1)-N(3)	-	93.75(12)	-	-	-
O(1)-Zn(2)-O(2)	77.94(11)	77.86(8)	76.65(10)	77.96(7)	77.27(8)
O(1)-Zn(2)-O(4)	149.40(10)	151.07(8)	149.75(10)	-	-
O(1)-Zn(2)-O(3)	-	-	-	72.87(7)	73.24(8)
O(1)-Zn(2)-O(5)	99.18(11)	-	97.94(11)	153.27(8)	155.90(10)
O(1)-Zn(2)-O(1)[a]	-	97.52(8)	-	-	-
O(1)-Zn(2)-O(6)	126.42(11)	-	116.55(10)	121.33(8)	120.52(9)
O(1)-Zn(2)-O(2)[a]	-	119.36(9)	-	-	-
O(1)-Zn(2)-O(8)	93.64(11)	-	91.88(10)	-	-
O(1)-Zn(2)-O(7)	-	-	-	87.71(7)	88.51(9)
O(1)-Zn(2)-O(4)[a]	-	95.45(8)	-	-	-
O(2)-Zn(2)-O(4)	71.49(10)	73.24(8)	73.20(11)	-	-
O(2)-Zn(2)-O(3)	-	-	-	150.49(8)	150.35(8)
O(2)-Zn(2)-O(5)	119.80(11)	-	119.46(11)	120.33(8)	119.22(8)
O(2)-Zn(2)-O(1)[a]	-	119.36(9)	-	-	-
O(2)-Zn(2)-O(6)	150.36(11)	-	157.78(11)	97.47(8)	95.32(9)
O(2)-Zn(2)-O(2)[a]	-	155.48(9)	-	-	-
O(2)-Zn(2)-O(8)	91.88(11)	-	88.98(11)	-	-
O(2)-Zn(2)-O(7)	-	-	-	93.08(7)	97.22(9)
O(2)-Zn(2)-O(4)[a]	-	88.61(8)	-	-	-
O(4)-Zn(2)-O(5)	94.85(10)	-	98.91(11)	-	89.83(8)

O(4)-Zn(2)-O(1)[a]	-	95.45(8)	-	-	-
O(4)-Zn(2)-O(6)	83.24(10)	-	91.49(11)	-	96.84(9)
O(3)-Zn(2)-O(5)	-	-	-	88.64(7)	-
O(3)-Zn(2)-O(6)	-	-	-	93.85(7)	-
O(4)-Zn(2)-O(2)[a]	-	88.61(8)	-	-	-
O(4)-Zn(2)-O(8)	88.73(10)	-	85.20(10)	-	-
O(4)-Zn(2)-O(7)	-	-	-	-	85.22(9)
O(3)-Zn(2)-O(7)	-	-	-	90.20(7)	-
O(4)-Zn(2)-O(4)[a]	-	85.24(8)	-	-	-
O(5)-Zn(2)-O(6)	76.60(10)	-	78.06(11)	78.06(7)	77.65(9)
O(1)[a]-Zn(2)-O(2)[a]	-	77.86(8)	-	-	-
O(5)-Zn(2)-O(8)	147.61(10)	-	151.32(10)	-	-
O(5)-Zn(2)-O(7)	-	-	-	72.90(7)	72.76(9)
O(1)[a]-Zn(2)-O(4)[a]	-	151.07(8)	-	-	v
O(6)-Zn(2)-O(8)	71.87(10)	-	73.46(10)	-	-
O(6)-Zn(2)-O(7)	-	-	-	150.56(7)	150.33(9)
O(2)[a]-Zn(2)-O(4)[a]	-	73.24(8)	-	-	-
O(5)-Zn(3)-O(6)	75.71(10)	-	76.31(11)	75.89(7)	76.39(9)
O(5)-Zn(3)-N(3)	92.63(13)	-	91.61(12)	88.83(8)	88.99(11)
O(5)-Zn(3)-N(4)	164.62(12)	-	162.39(13)	131.29(8)	133.67(9)
O(5)-Zn(3)-N(6)	-	-	101.28(14)	-	-

O(5)-Zn(3)-N(8)	97.73(14)	-	-	118.30(9)	117.04(13)
O(6)-Zn(3)-N(3)	120.19(13)	-	136.13(12)	162.53(8)	160.90(11)
O(6)-Zn(3)-N(4)	89.00(13)	-	89.61(13)	91.13(8)	91.33(10)
O(6)-Zn(3)-N(6)	-	-	109.60(14)	-	-
O(6)-Zn(3)-N(8)	125.22(14)	-	-	101.43(9)	103.83(11)
N(3)-Zn(3)-N(4)	93.74(15)	-	91.36(15)	92.74(9)	90.00(11)
N(3)-Zn(3)-N(6)	-	-	114.12(15)	-	-
N(3)-Zn(3)-N(8)	114.35(16)	-	-	93.19(9)	93.69(12)
N(4)-Zn(3)-N(6)	-	-	93.32(15)	-	-
N(4)-Zn(3)-N(8)	92.36(15)	-	-	110.22(10)	109.24(13)

Symmetry transformations: ^{a} = 1-x,y,3/2-z.

Supramolecular interactions

Diverse supramolecular architectures have been observed in the solid state structures of the complexes (**1**-**5**). These structures have been stabilized by non-covalent interactions mainly via; hydrogen bonding and C-H···π interactions.

In complex **1**, two intermolecular hydrogen bonding and two C-H···π interactions are observed. Hydrogen atoms, H(1N) and H(3N), attached to amine nitrogen atoms, N(1) and N(3), respectively, form intermolecular hydrogen bonds with symmetry related azide nitrogen atom, N(5)^{a} and N(8)^{b}, respectively {Symmetry transformation: ^{a} = 1-x,1-y,-z and ^{b} = 2-x,1-y,1-z}. The distance between the donor···acceptor is 3.006(6) Å and 2.981(6) Å for N(1)···N(5) and N(1)···N(8) respectively. Hydrogen atoms, H(9A) and H(21C), attached with carbon atoms, C(9) and C(21), respectively have been involved in intramolecular C-H···π interactions with phenyl rings, Cg(13) and Cg(14) respectively. The measured C-H···π interaction distances are 3.480(5) Å for C(9)-H(9A)···Cg(13) and 3.868(8) Å for C(21)-H(21C)···Cg(14). These interactions result in a one-dimensional array shown in Fig. S1.

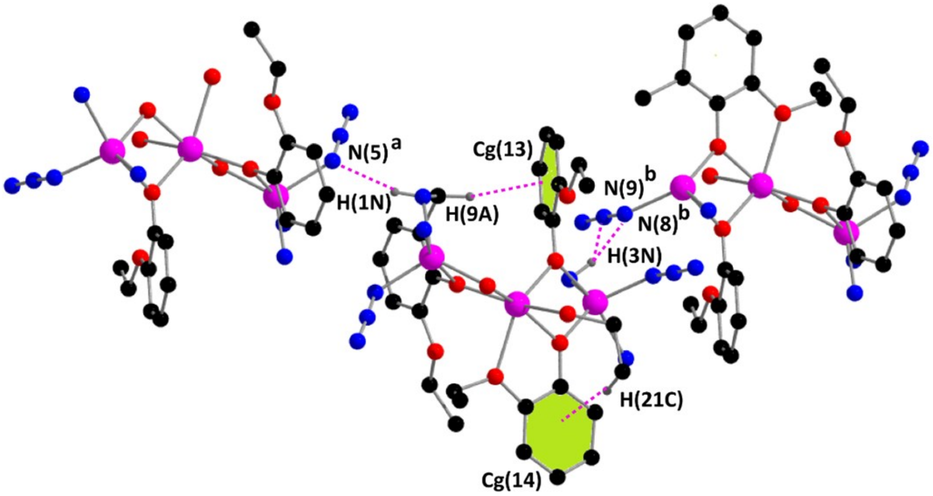

Fig. S1. Prespective view of hydrogen bonding and C-H···π interactions in complex **1**. Only the relevant atoms have been shown for clarity.

In complex **2**, the hydrogen atom, H(1N), attached to the amine nitrogen atom, N(1), is involved in an intermolecular hydrogen bonding interaction with the symmetry related nitrogen atom, N(3), {Symmetry transformation: ^{c} = 1-x,1-y,1-z} of a thiocyanate molecule. The distance between the donor···acceptor is 3.167(4) Å for N(1)···N(3). The hydrogen atom, H(9A), attached with carbon atom, C(9), has been involved in an intramolecular C-H···π interaction with the symmetry related phenyl ring, Cg(8)^{h}, {Symmetry transformation: ^{h} = 1-x,y,3/2-z}. The C-H···π interaction distance is 3.761(4) Å for C(9)-H(9A)···Cg(8). A one-dimensional structure has been formed as a combination of these interactions shown in Fig S2.

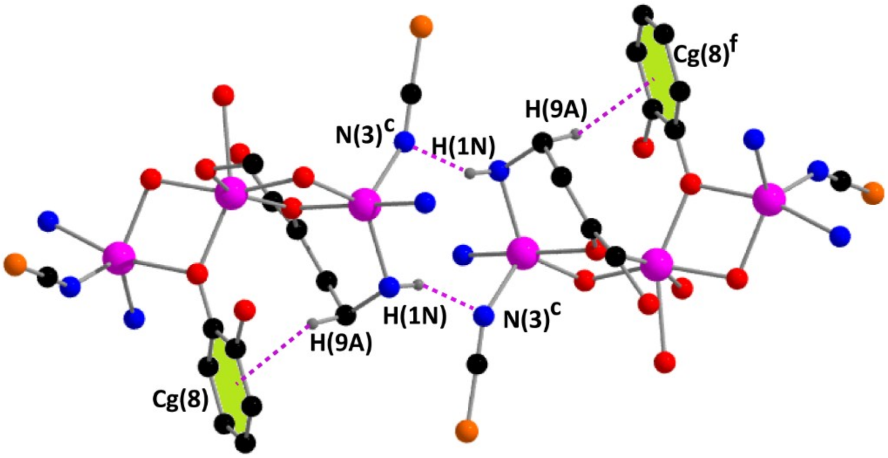

Fig. S2. Prespective view of hydrogen bonding and C-H···π interactions in complex **2**. Only the relevant atoms have been shown for clarity.

In complex **3**, hydrogen atoms, H(1) and H(3A), attached to amine nitrogen atoms, N(1) and N(3), have been involved in intermolecular hydrogen bonding interactions with symmetry related nitrogen atoms, N(5)^c and N(6)^a {Symmetry transformation: ^{c} = 1-x,1-y,1-z and ^{a} = 1-x,1-y,-z} of two thiocyanate molecules. Dimensions are 3.006(6) Å for N(1)···N(5) and 2.981(6) Å for N(3)···N(6). Hydrogen atoms, H(1A) and H(8B), attached with carbon atoms, C(1) and C(8), are involved in intramolecular C-H···π interactions with phenyl rings, Cg(14) and Cg(13) respectively. Again hydrogen atoms, H(11B) and H(33C), attached with carbon atoms, C(11) and C(33) have been involved in intermolecular C-H···π interactions with symmetry related phenyl rings, Cg(11)^c and Cg(13)^a respectively {Symmetry transformation: ^{c} = 1-x,1-y,1-z and ^{a} = 1-x,1-y,-z}. C-H···π interaction distances are 3.464(6) Å for C(1)−H(1A)···Cg(14), 3.891(6) Å for C(8)−H(8B)···Cg(13), 3.658(6) Å for C(11)−H(11B)···Cg(11) and 3.530(7) Å for C(33)−H(33C)···Cg(13). As a result of these interactions a 1-D structure is formed shown in Fig. S3.

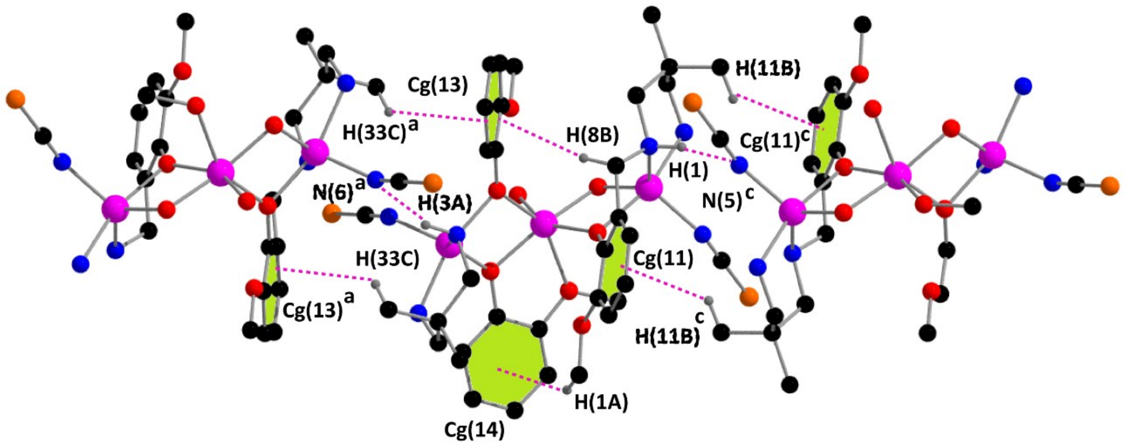

Fig. S3. Prespective view of hydrogen bonding and C-H···π interactions in complex **3**. Only the relevant atoms have been shown for clarity.

In complex **4**, the hydrogen atom, H(2N), attached to amine nitrogen atom, N(2), is involved in two intermolecular hydrogen bonding interactions with symmetry related two nitrogen atoms N(5)^d and N(6)^d of an azide molecule {Symmetry transformation: ^{d} =1-x,1-y,2-z}. Similarly, hydrogen atom, H(3N), attached to amine nitrogen atom, N(3), forms an intermolecular hydrogen bonding interaction with the symmetry related nitrogen atoms N(8)^e of an azide molecule {Symmetry transformation: ^{e} = -x,1-y,1-z}. Dimensions are donor···acceptor are 3.031(3) Å for N(2)···N(5), 3.260(3) Å for N(2)···N(6) and 3.082(3) Å for N(3)···N(8). Three intramolecular C−H···π interactions are also observed where the hydrogen atoms, H(14B), H(21A) and H(35A) attached with the carbon atoms C(14), C(21) and C(35) respectively have been involved in three intramolecular C−H···π interactions with phenyl rings, Cg(14), Cg(13) and Cg(12) respectively. The measured C−H···π interaction distances are 3.848(3) Å for C(14)−H(14B)···Cg(14), 3.690(5) Å for C(21)−H(21A)···Cg(13) and 3.834(3) Å for C(35)−H(35A)···Cg(12). The interactions resulted in one dimension structure shown in Fig. S4.

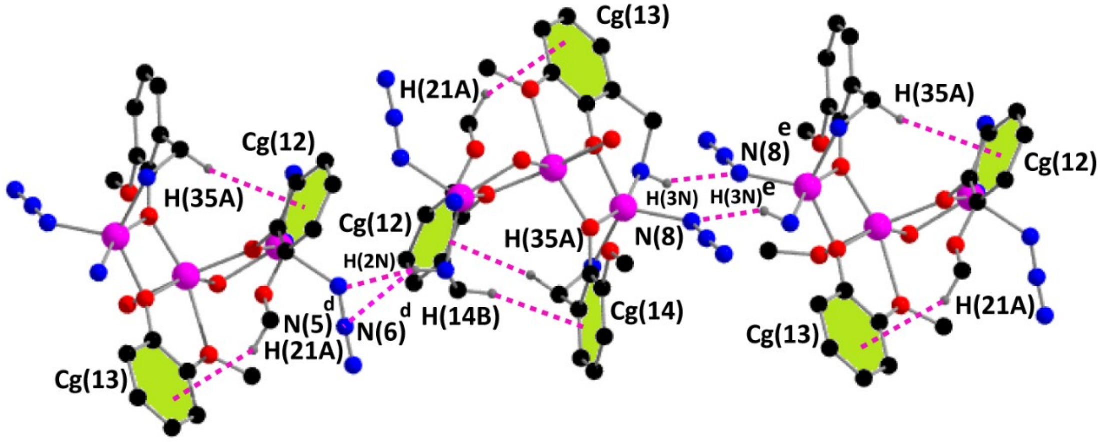

Fig. S4. Prespective view of hydrogen bonding and C-H···π interactions in complex **4**. Only the relevant atoms have been shown for clarity.

In complex **5**, the hydrogen atoms, H(2N) and H(4N), attached to amine nitrogen atoms, N(2) and N(4), have been intricate in intermolecular hydrogen bonding interactions with symmetry related nitrogen atoms, N(5)^{f} and N(8)^{g} {Symmetry transformation: ^{f} =1-x,-y,-z and ^{g} =1-x,-y,1-z } of an azide molecule. The distances between the donor···acceptor are 3.099 (4) Å for N(2)···N(5), 3.062(4) Å for N(4)···N(8). Again, the hydrogen atoms, H(12B) and H(35C), attached with carbon atoms C(12) and C(33), have been involved in two intermolecular C-H···π interactions with symmetry related phenyl rings, Cg(12)^{f}, Cg(13)^{d} respectively {Symmetry transformation: ^{f} = 1-x,-y,-z and ^{d} **=** 1-x,1-y,2-z} whereas two other hydrogen atoms, H(22A) and H(25B), attached with carbon atoms, C(22) and C(25) are involved in two intramolecular C-H···π interactions with phenyl rings, Cg(14) and Cg(11) respectively. The measured distances are 3.527(4) Å for C(12)−H(12B)···Cg(12), 3.501(5) Å for C(22)−H(22A)···Cg(14), 3.703(7) Å for C(25)−H(25B)···Cg(11) and 3.512(4) Å for C(35)−H(35C)···Cg(13). A one-dimensional array has been formed and shown in Fig. S5. The details of the geometric features of the hydrogen bonding and C−H···π interactions are given in Tables S3 and S4 respectively.

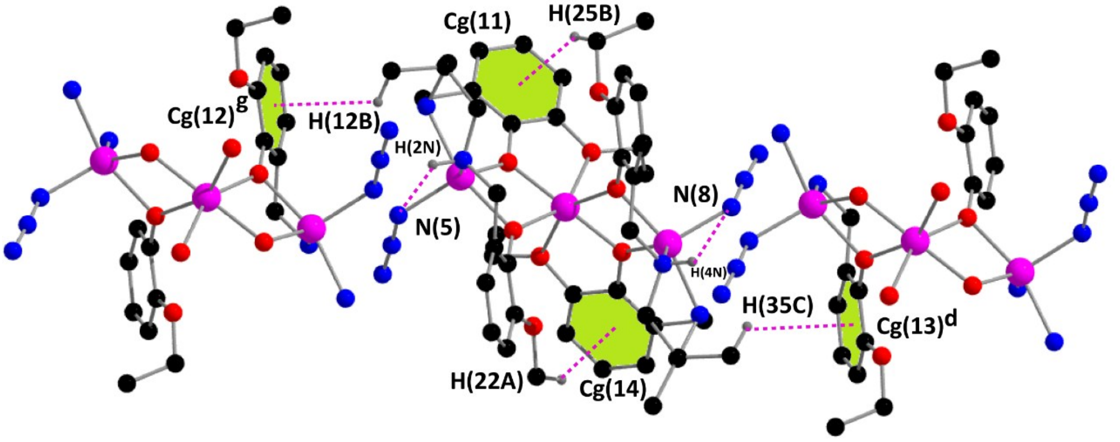

Fig. S5. Prespective view of hydrogen bonding and C-H···π interactions in complex **5**. Only the relevant atoms have been shown for clarity.

Table S3: Hydrogen bond distances (A˚) and angles (°) for complexes **2** and **3**.

Complex	D-H···A	H···A (Å)	D-H (Å)	D···A (Å)	∠D-H···A
1	N(1)-H(1N)···N(5)[a]	2.18(4)	0.87(4)	3.006(6)	158(3)
	N(3)-H(3N)···N(8)[b]	2.09(4)	0.92(4)	2.981(6)	162(3)
2	N(1)-H(1N)···N(3)[c]	2.42(4)	0.81(4)	3.167(4)	153(3)
3	N(1)-H(1)···N(5)[c]	2.33	0.98	3.246(6)	155.0
	N(3)-H(3A)···N(6)[a]	2.37	0.98	3.279(6)	153.0
4	N(2)-H(2N)···N(5)[d]	2.19(3)	0.87(3)	3.031(3)	162(3)
	N(2)-H(2N)···N(6)[d]	2.55(3)	0.87(3)	3.260(3)	139(3)
	N(3)-H(3N)···N(8)[e]	2.35(3)	0.82(3)	3.082(3)	148(2)
5	N(2)-H(2N)···N(5)[f]	2.29(4)	0.87(4)	3.099(4)	154(4)
	N(4)-H(4N)···N(8)[g]	2.27(4)	0.86(4)	3.062(4)	154(4)

Symmetry transformations : ^{a} = 1-x,1-y,-z; ^{b} = 2-x,1-y,1-z; ^{c}=1-x,1-y,1-z; ^{d} =1-x,1-y,2-z; ^{e} = -x,1-y,1-z; ^{f} =1-x,-y,-z ; ^{g} = 1- x,- y, 1- z.

Table S4: Geometric features (distances in Å and angles in°) of the C-H···π interactions obtained for complexes **1** and **2**.

Complex	**C-H···Cg(Ring)**	**H···Cg (Å)**	**C-H···Cg (°)**	**C···Cg (Å)**
1	C(9)-H(9A)···Cg(13)	2.55	160	3.480(5)
	C(21)-H(21C)···Cg(14)	2.93	167	3.868(8)
2	C(9)-H(9A)···Cg(8)^{g}	2.83	161	3.761(4)
3	C(1)-H(1A)···Cg(14)	2.72	135	3.464(6)
	C(8)-H(8B)···Cg(13)	2.96	163	3.891(6)
	C(11)-H(11B)···Cg(11)^{c}	2.96	130	3.658(6)
	C(33)-H(33C)···Cg(13)^{a}	2.99	117	3.530(7)
4	C(14)-H(14B)···Cg(14)	2.90	167	3.848(3)
	C(21)-H(21A)···Cg(13)	2.93	137	3.690(5)
	C(35)-H(35A)···Cg(12)	2.90	163	3.834(3)
5	C(12)-H(12B)···Cg(12)^{f}	2.96	119	3.527(4)
	C(22)-H(22A)···Cg(14)	2.67	143	3.501(5)
	C(25)-H(25B)···Cg(11)	2.86	146	3.703(7)
	C(35)-H(35C)···Cg(13)^{d}	2.89	123	3.512(4)

Symmetry transformations: ^{a} = 1-x,1-y,-z; ^{c}=1-x,1-y,1-z; ^{d} =1-x,1-y,2-z; ^{f} =1-x,-y,-z.

Cg(13) = Centre of gravity of the ring [C(24)–C(25)–C(26)–C(27)–C(28)–C(29)]; Cg(14) = Centre of gravity of the ring [C(35)–C(36)–C(37)–C(38)–C(39)–C(40)] for complex **1**. Cg(8) = Centre of gravity of the ring [C(3)–C(4)–C(5)–C(6)–C(7)–C(8)] for complex **2**. Cg(8) = Centre of gravity of the ring [C(3)–C(4)–C(5)–C(6)–C(7)–C(8)]; Cg(14) = Centre of gravity of the ring [C(36)–C(37)–C(38)–C(39)–C(40)–C(41)]; Cg(13) = Centre of gravity of the ring [C(23)–C(24)–C(25)–C(26)–C(27)–C(28)]; Cg(11) = Centre of gravity of the ring [C(2)–C(3)–C(4)–C(5)–C(6)–C(7)] for complex **3**. Cg(14) = Centre of gravity of the ring [C(36)–C(37)–C(38)–C(39)–C(40)–C(41)]; Cg(13) = Centre of gravity of the ring [C(26)–C(27)–C(28)–C(29)–C(30)–C(31)]; Cg(12) = Centre of gravity of the ring [C(15)–C(16)–C(17)–C(18)–C(19)–C(20)] for complex **4**. Cg(11) = Centre of gravity of the ring [C(3)–C(4)–C(5)–C(6)–C(7)–C(8)]; Cg(12) = Centre of gravity of the ring [C(16)–C(17)–C(18)–C(19)–C(20)–C(21)]; Cg(13) = Centre of gravity of the ring [C(26)–C(27)–C(28)–C(29)–C(30)–C(31)]; Cg(14) = Centre of gravity of the ring [C(39)–C(40)–C(41)–C(42)–C(43)–C(44)] for complex **5**.

Hirshfeld surfaces

The Hirshfeld surface emerged from an attempt to define the space occupied by a molecule in a crystal for the purpose of subdividing the crystal electron density into molecular fragments.[3] d_{norm} is a normalised contact distance.[4] Intermolecular contacts are highlighted in the d_{norm} surface (when atoms make intermolecular contacts closer than the sum of their van der Waals radii, these contacts will be highlighted in red whereas longer contacts are blue, and contacts around the sum of van der Waals radii are white). Hirshfeld surfaces of complexes **1**-**5**, mapped over d_{norm} (range of -0.1 to 1.5 Å), is illustrated in Fig. S6. Red spots on these surfaces denote the dominant interactions [N···H/H···N, S···H/H···S and O···H/H···O].

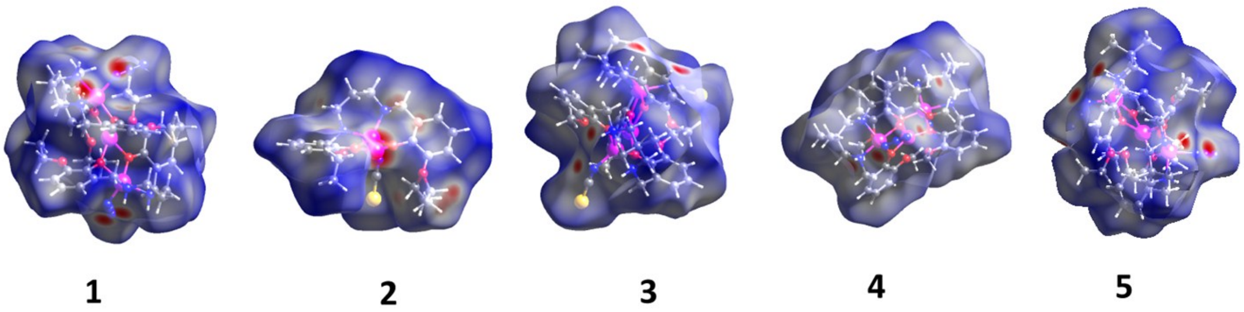

Fig. S6. Hirshfeld surfaces of complexes **1**-**5** mapped over $d_{norm.}$

As the Hirshfeld surface defines the shape of the molecule in terms of its surrounding crystalline environment, the local shape of the surface may provide some chemical insight whereas shape index is a qualitative measure of shape and can be sensitive to very subtle changes in surface shape, particularly in regions where the total curvature (or the curvedness) is very low.[5] Hirshfeld surfaces of complexes **1**-**5**, mapped over shape index and curvedness (range of -0.1 to 1.5 Å), are illustrated in Fig. S7 and S8 respectively.

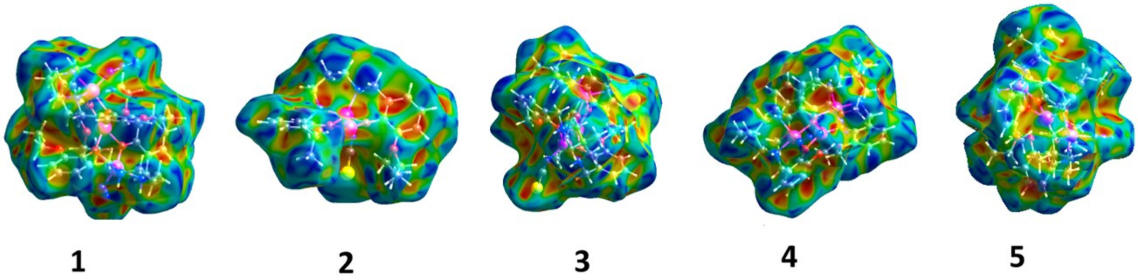

Fig. S7. Hirshfeld surfaces of complexes **1**-**5** mapped over shape index.

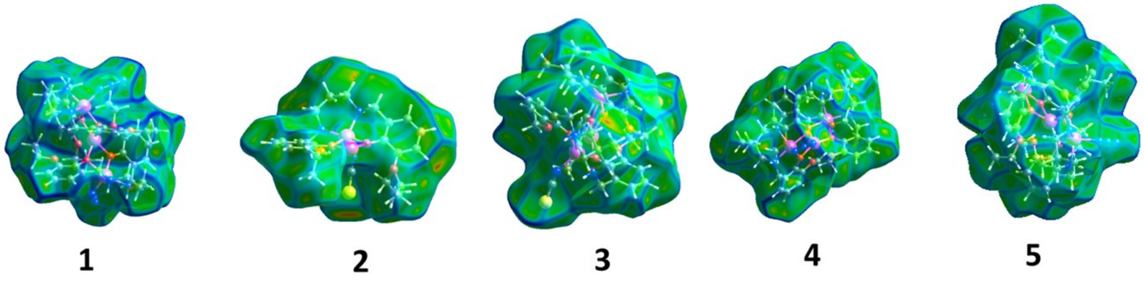

Fig. S8. Hirshfeld surfaces of complexes **1**-**5** mapped over curvedness.

The 2D fingerprint plots,[6] which are used to analyze the intermolecular contacts at the same time, revealed that the main intermolecular interactions in the complexes are S···H/H···S, N···H/H···N or O···H/H···O shown in Fig. S9.

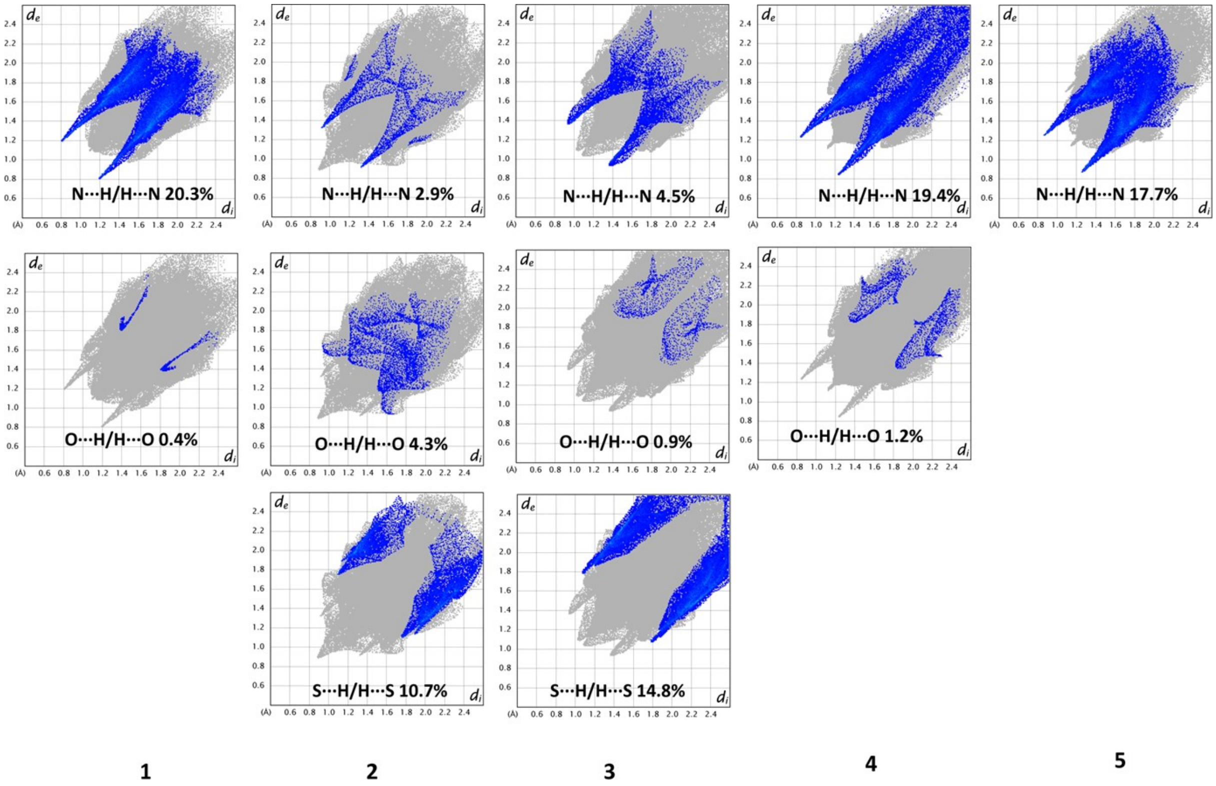

Fig. S9. Fingerprint plot: Different contacts contributed to the total Hirshfeld Surface area of complexes **1**-**5**.

IR and electronic spectra

Strong bands around 2032-2059 cm^{-1} indicate the presence of terminal N-bonded azide in complexes **1**, **4**, **5** and N-bonded thiocyanate in complexes **2** and **3**.[7] Broad bands around 3240-3180 cm^{-1} indicate the presence of amine N-H stretching.[8] Broad bands in the range of

2923-2888 cm^{-1} due to alkyl C-H stretching vibrations are routinely noticed in IR spectra of the complexes.[9]

Electronic spectra of the complexes consist of two bands. One ~288 nm and the other ~375 nm which may be assigned as intra ligand charge transfer transitions.[10] All complexes exhibit fluorescence in DMF solution upon excitation at 288 nm. The emissions occur ~415 nm which may be assigned as intra-ligand charge transfer fluorescence. The UV-Vis and fluorescence spectra of the complexes are shown in Fig. S10. The fluorescence data are listed in Table S5 (without solvent corrections). Mean lifetimes (r_{avg}) of the exited states are listed in Table S5. Decay profiles are shown in Fig. S11.

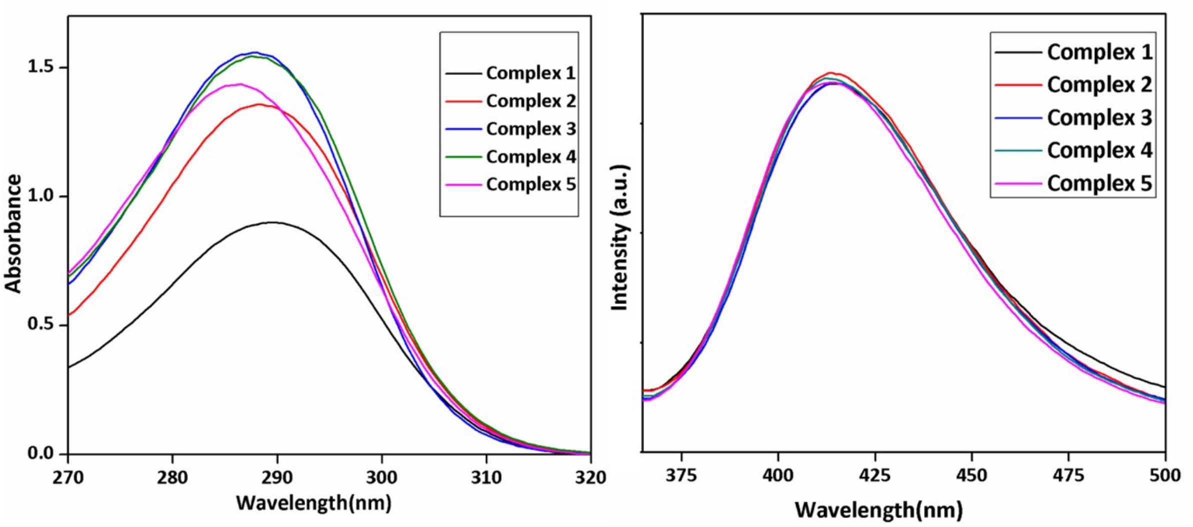

(a)

(b)

Fig. S10. (a) UV-Vis spectra of 10^{-5} M solution of all complexes; (b) Fluorescence spectra of all complexes (upon excitation at 288 nm, conc. 10^{-5} M) in DMF.

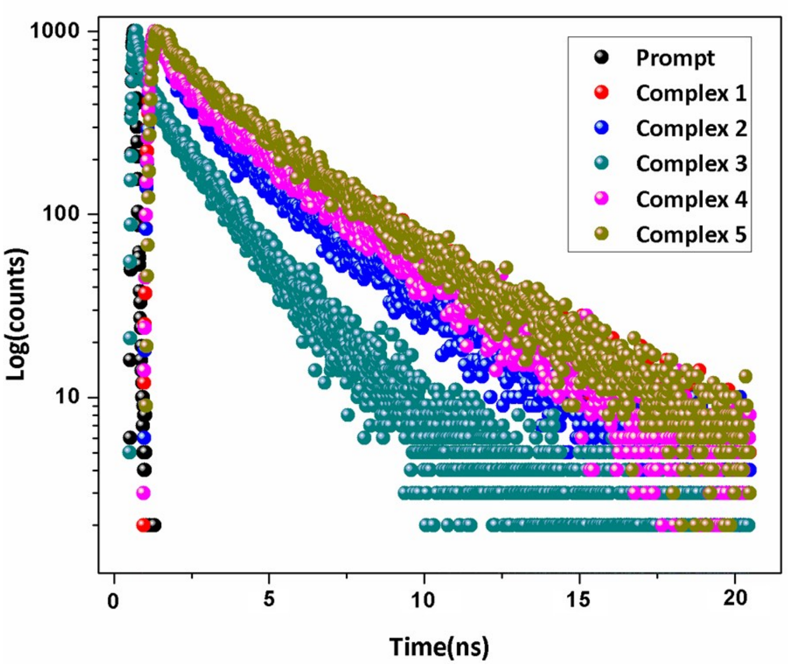

Fig. S11. Lifetime decay profile of complexes **1**-**5**.

Table S5: Photophysical data for complexes **1**-**5**.

Complex	**Absorption (nm)**	**Emission (nm)**	**A_1 (%)**	**τ_1(ns)**	**A_2 (%)**	**τ_2(ns)**	**τ_{avg} (ns)**	**χ^2**
1	288	415	13.44	2.33	86.56	10.08	9.81	1.08
2	288	416	29.76	2.21	70.24	9.68	9.01	1.09
3	288	414	17.83	1.83	82.17	11.25	10.92	1.12
4	288	417	13.62	1.47	86.38	9.83	9.64	1.04
5	288	415	12.82	3.51	87.18	11.02	8.89	1.04

Powder X-ray diffraction and Mass Spectra

The experimental powder XRD patterns of bulk product of complexes are in good agreement with simulated XRD pattern from single crystal X-ray diffraction, confirming purity of the bulk samples [Fig. S12]. The simulated pattern of the complexes have been calculated from the different single crystal structural data (cif files) using the CCDC Mercury software.

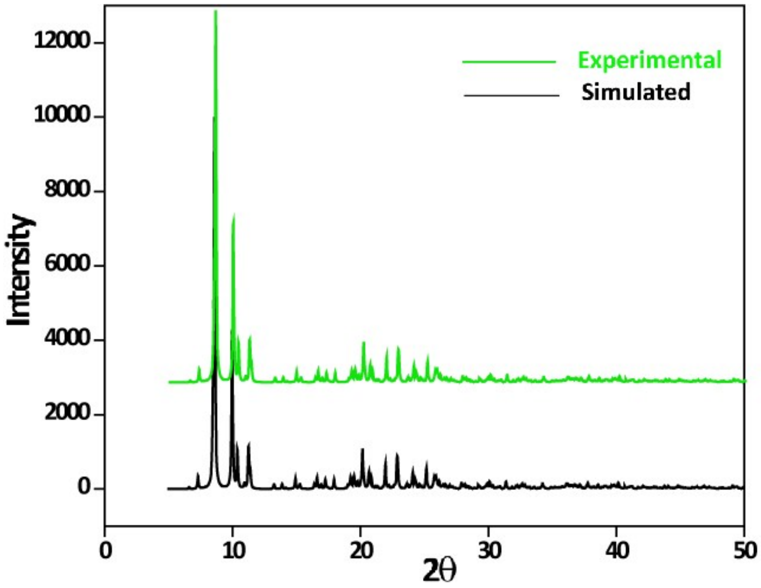

Fig. S12: Experimental and simulated PXRD patterns of complex **1** confirming purity of the bulk material.

The mass spectral analyses reveal that the complexes break in DMF. The mass spectrum of complex **3** shows base peaks at m/z 877.2526, 545.0479 and 375.1876 which can be assigned to $[(L^2Zn)_2(H)]^+$, $[L^2Zn(CH_3OH)Na(H_2O)]$ and $[H_2L^2(H)]^+$ respectively. The mass spectrum of complex **4** shows base peaks at m/z 982.1578 and 375.2210 which can be assigned to $[(L^2)_2Zn_3N_3]^+$, and $[H_2L^2(H)]^+$ respectively. Peaks at m/z 982.0938 $[(L^1)_2Zn_3N_3]^+$, 875.1821

$[(L^1Zn)_2(H)]^+$ and 375.1973 $[H_2L^1(H)]^+$ has been observed for complex **1**. The mass spectra of complexes **1, 3** and **4** are shown in Figures S13-S15 respectively.

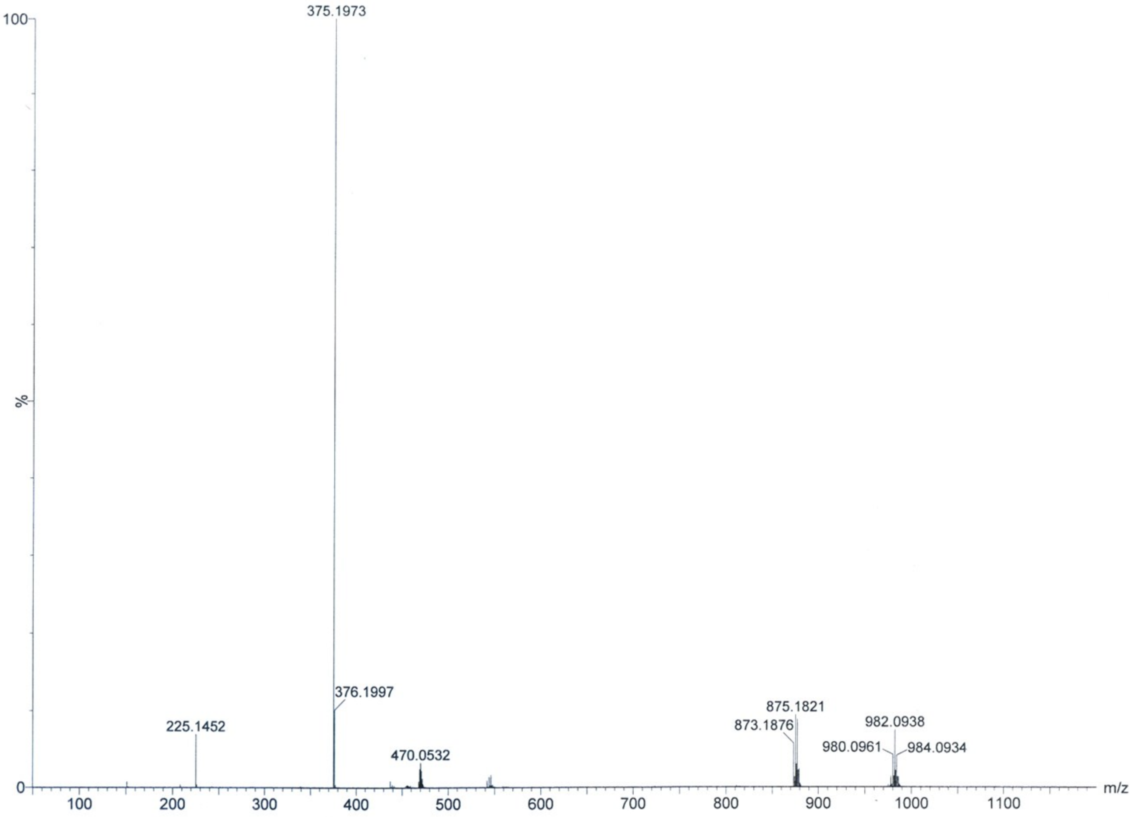

Fig. S13. Mass spectrum of complex **1**.

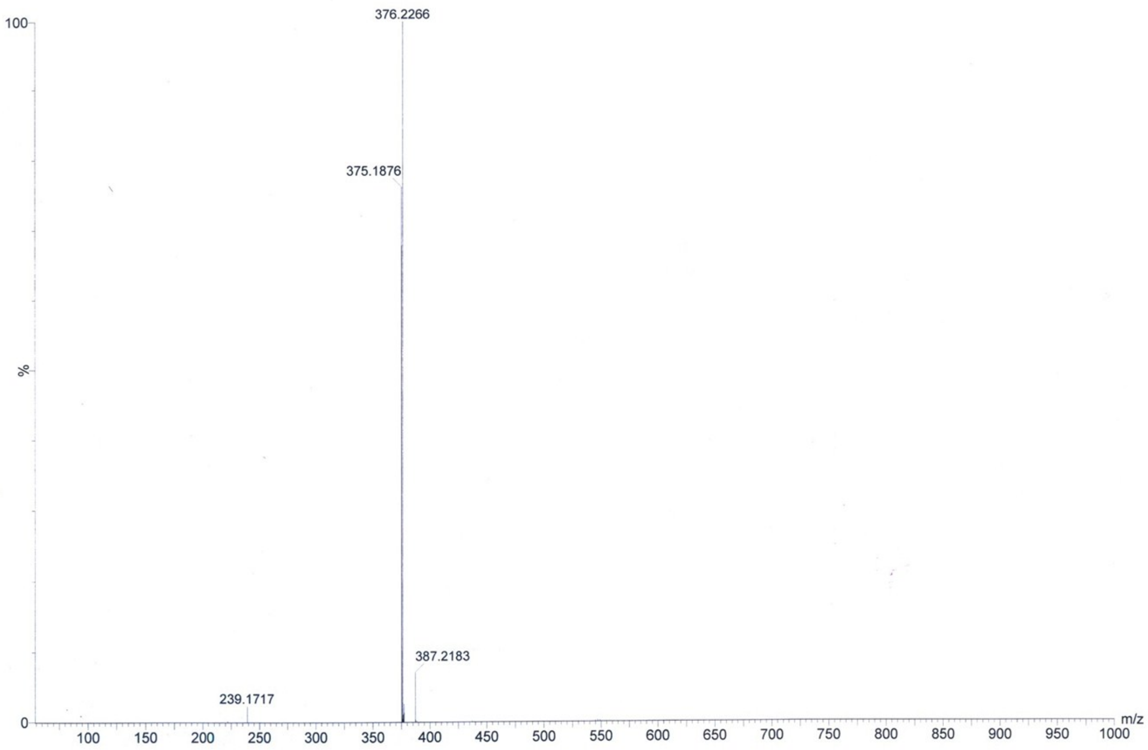

Fig. 14(a). Mass spectrum of complex **3** (Full scale).

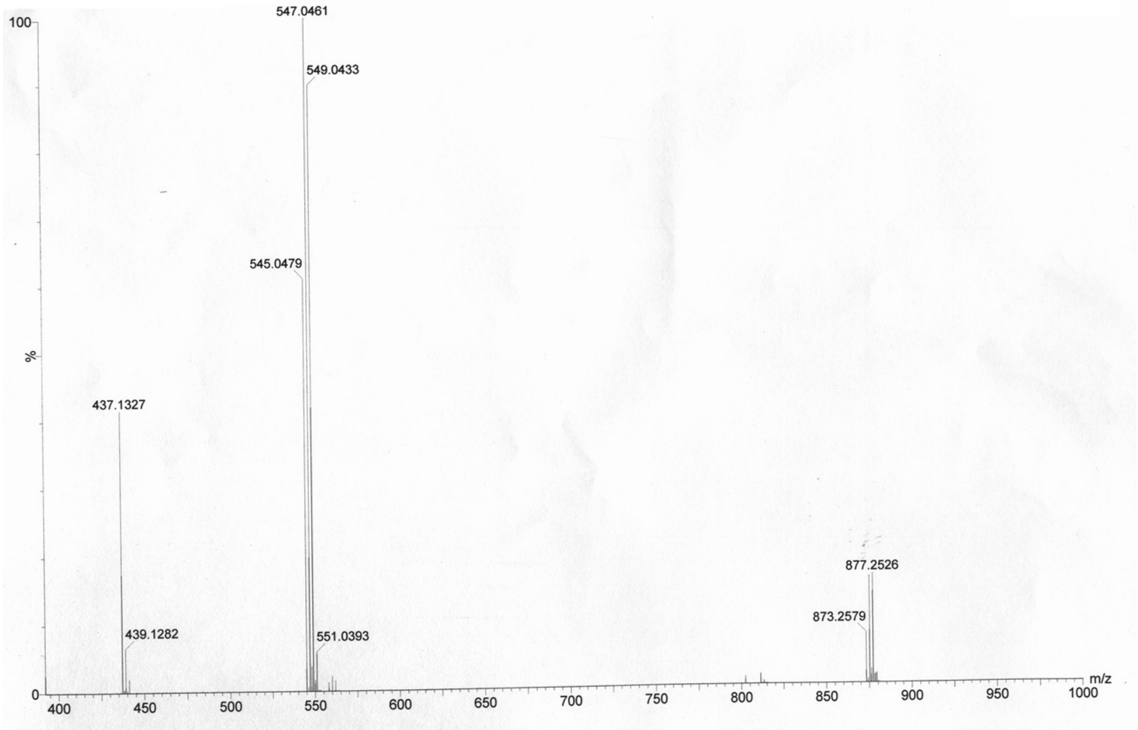

Fig. 14(b). Mass spectrum of complex **3** (Selected range 400-1000).

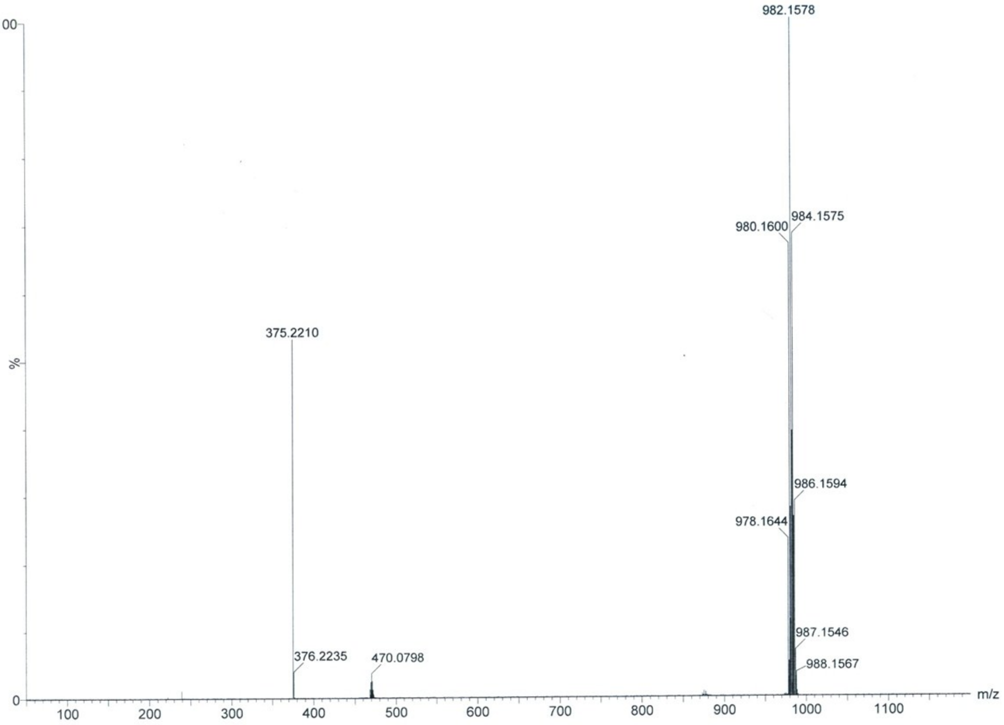

Fig. S15. Mass spectrum of complex **4**.

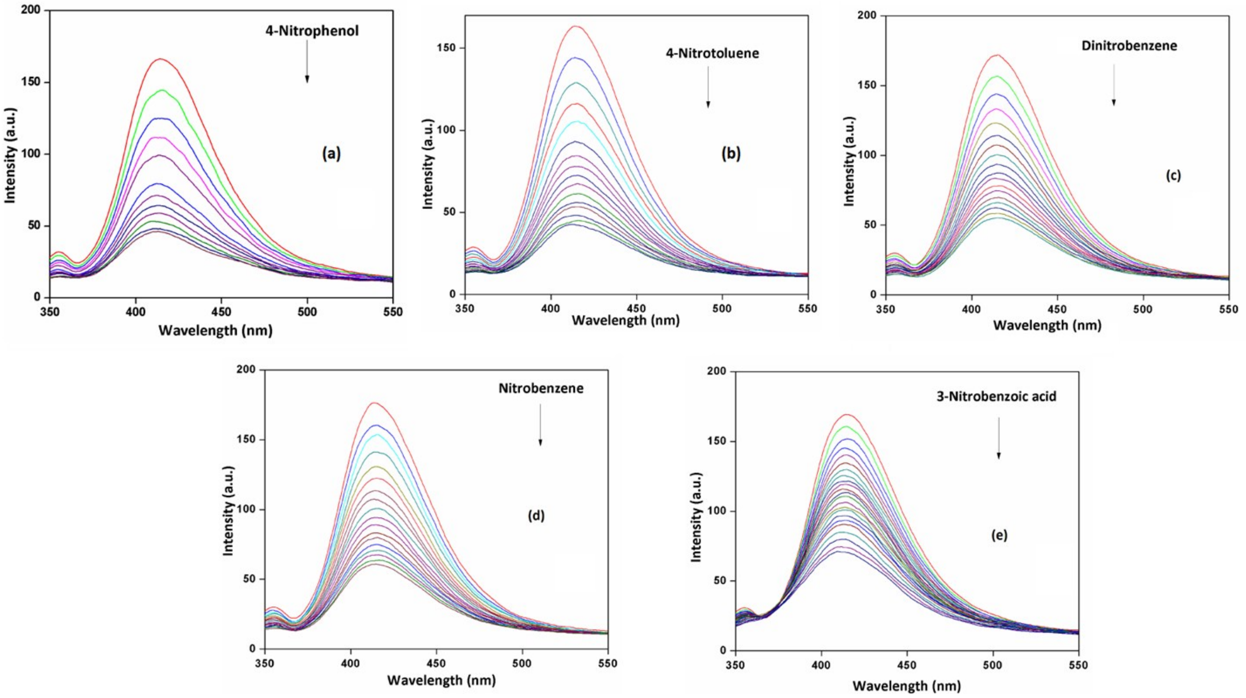

Fig. S16: Fluorescence spectra of complex **1** in DMF (excitation wavelength 288 nm and conc. 10^{-5} M) upon increasing concentration of 4-nitrophenol (a), 4-nitrotoluene (b), dinitrobenzene (c), nitrobenzene (d), 3-nitrobenzoic acid (e).

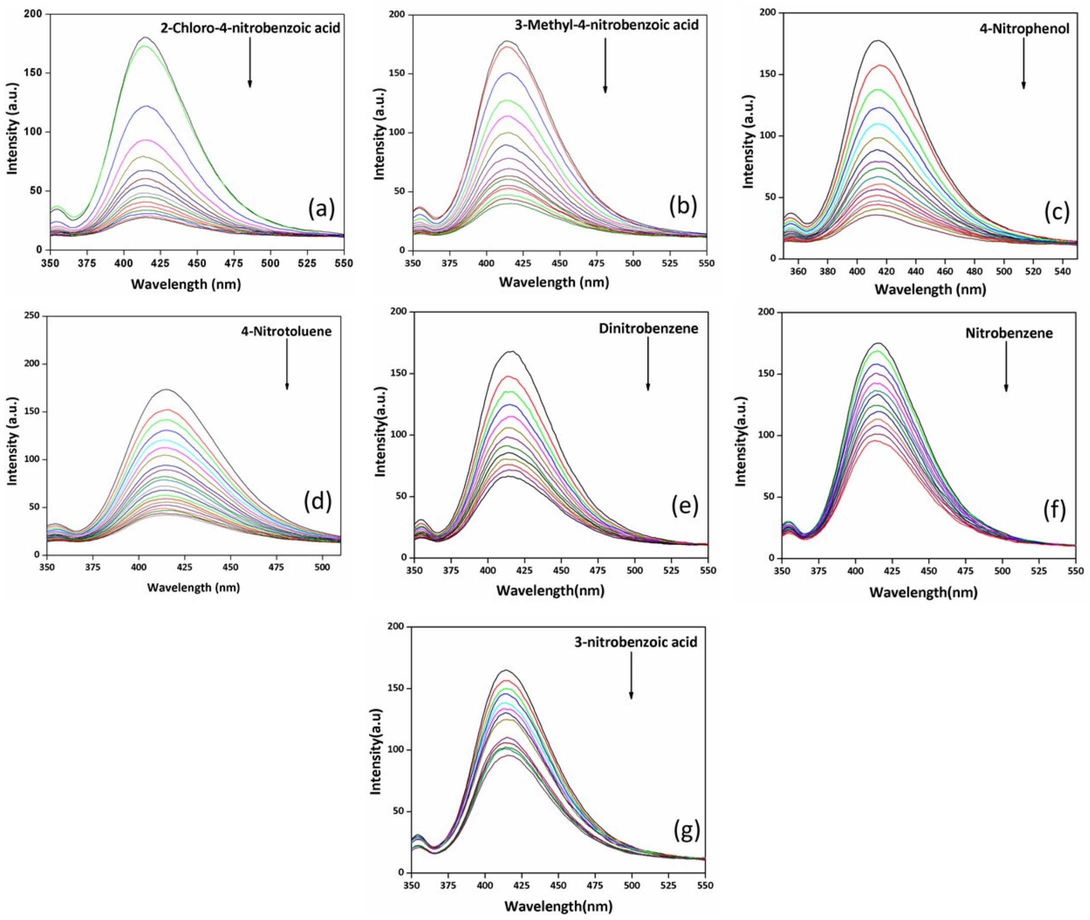

Fig. S17: Fluorescence spectra of complex **2** in DMF (excitation wavelength 288 nm and conc. 10^{-5} M) upon increasing concentration of 2-chloro-4-nitrobenzoic acid (a), 3-methyl-4-nitrobenzoic acid (b), 4-nitrophenol (c), 4-nitrotoluene (d), dinitrobenzene (e), nitrobenzene (f), 3-nitrobenzoic acid (g).

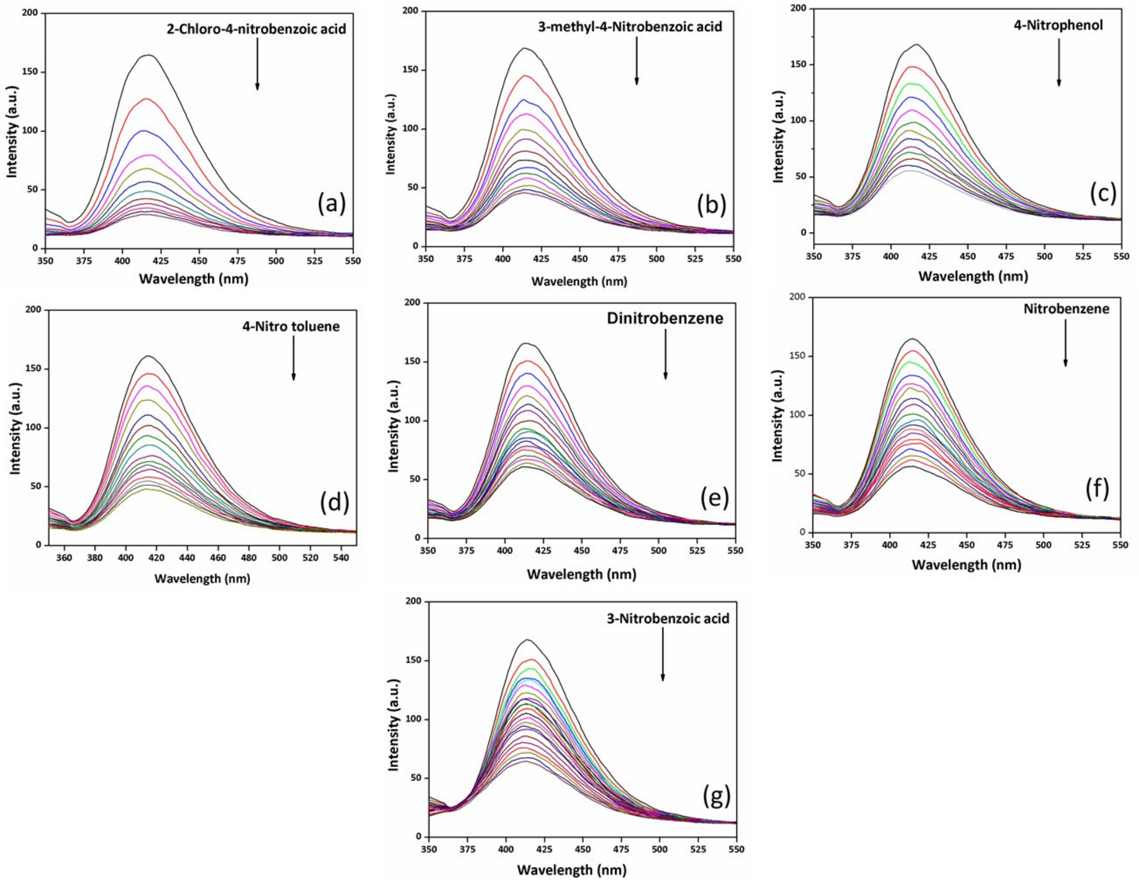

Fig. S18: Fluorescence spectra of complex **3** in DMF (excitation wavelength 288 nm and conc. 10^{-5} M) upon increasing concentration of 2-chloro-4-nitrobenzoic acid (a), 3-methyl-4-nitrobenzoic acid (b), 4-nitrophenol (c), 4-nitrotoluene (d), dinitrobenzene (e), nitrobenzene (f), 3-nitrobenzoic acid (g).

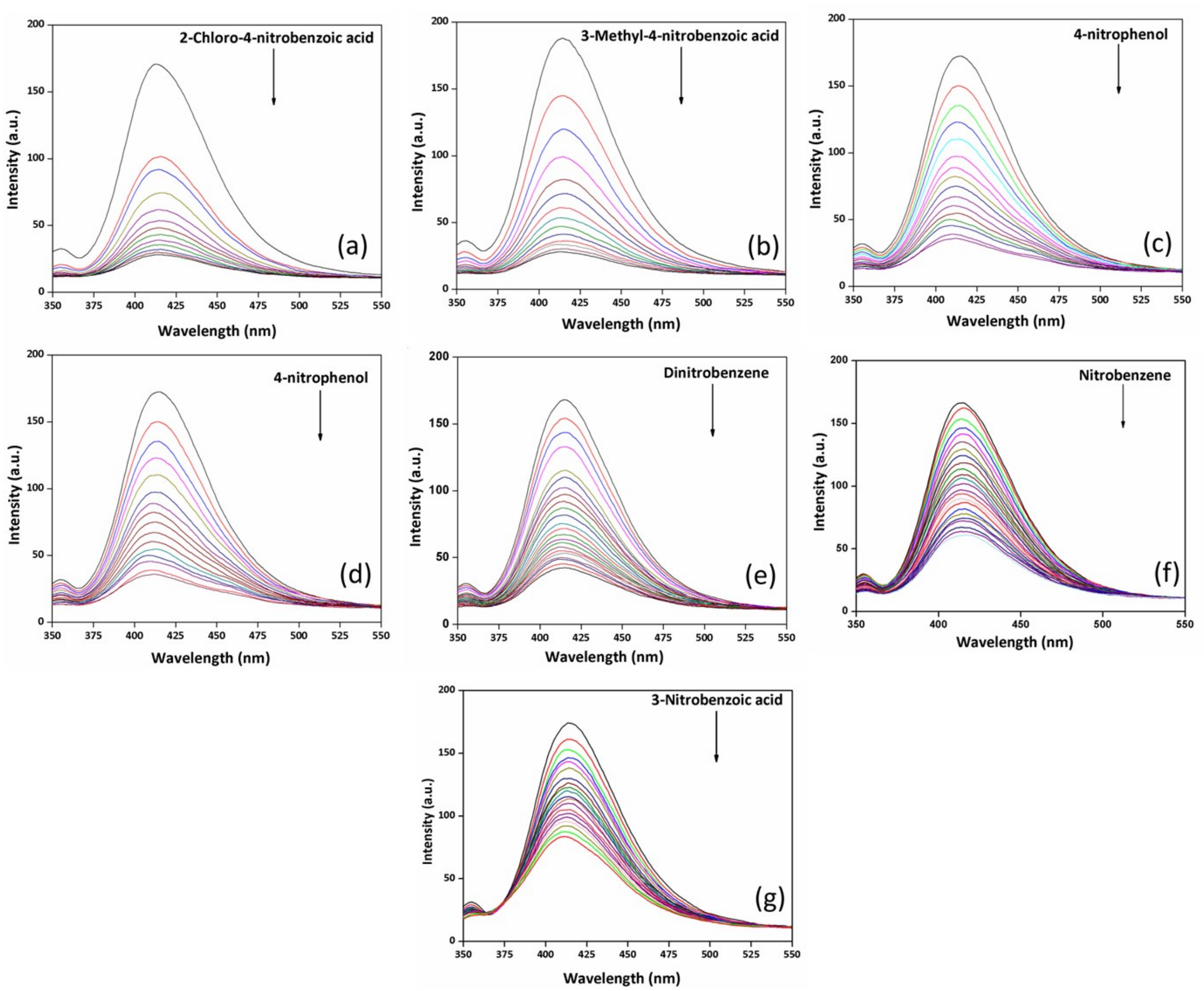

Fig. S19: Fluorescence spectra of complex **4** in DMF (excitation wavelength 288 nm and conc. 10^{-5} M) upon increasing concentration of 2-chloro-4-nitrobenzoic acid (a), 3-methyl-4-nitrobenzoic acid (b), 4-nitrophenol (c), 4-nitrotoluene (d), dinitrobenzene (e), nitrobenzene (f), 3-nitrobenzoic acid (g).

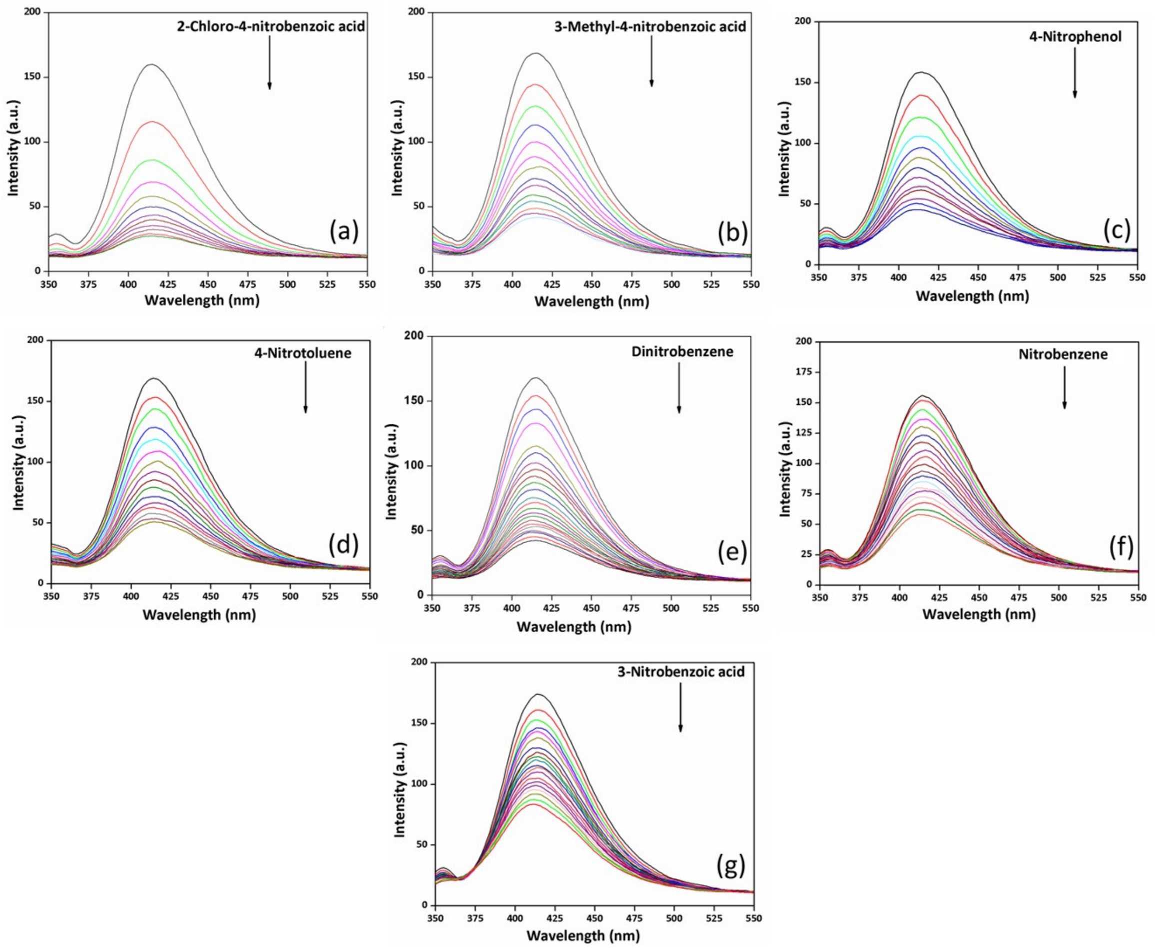

Fig. S20: Fluorescence spectra of complex **5** in DMF (excitation wavelength 288 nm and conc. 10^{-5} M) upon increasing concentration of 2-chloro-4-nitrobenzoic acid (a), 3-methyl-4-nitrobenzoic acid (b), 4-nitrophenol (c), 4-nitrotoluene (d), dinitrobenzene (e), nitrobenzene (f), 3-nitrobenzoic acid (g).

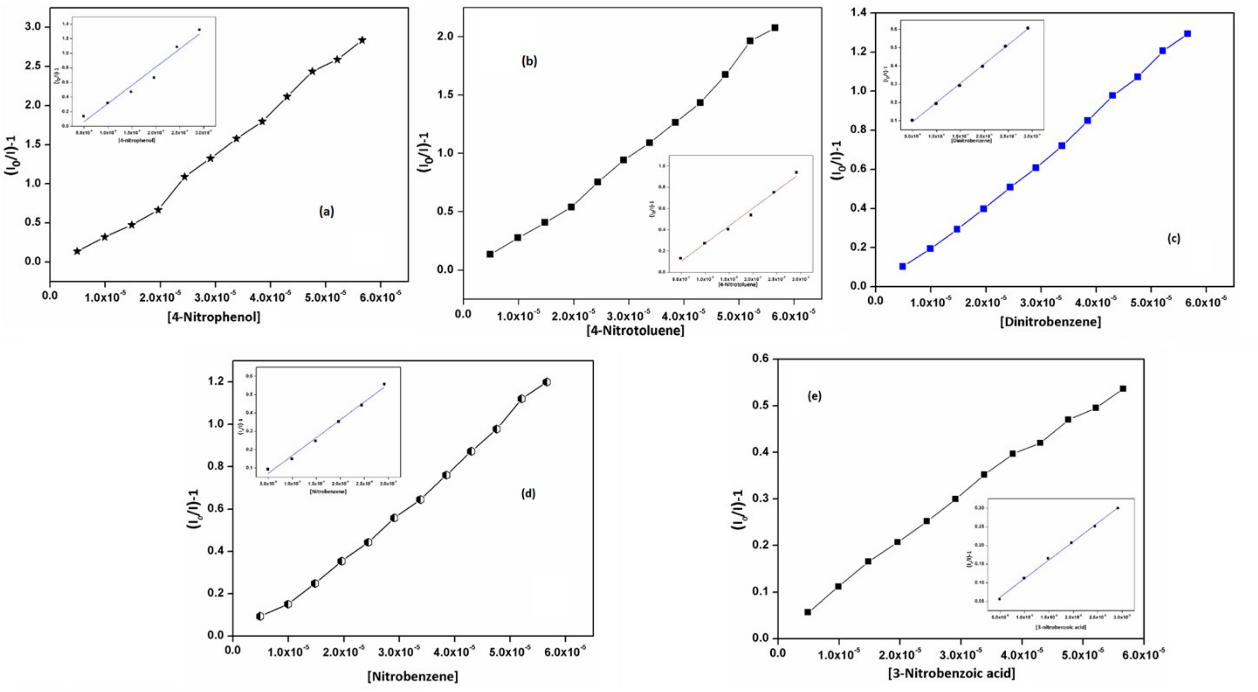

Fig. S21: Stern-Volmer plot of complex **1** with 4-nitrophenol (a), 4-nitrotoluene (b), dinitrobenzene (c), nitrobenzene (d), 3-nitrobenzoic acid in DMF.

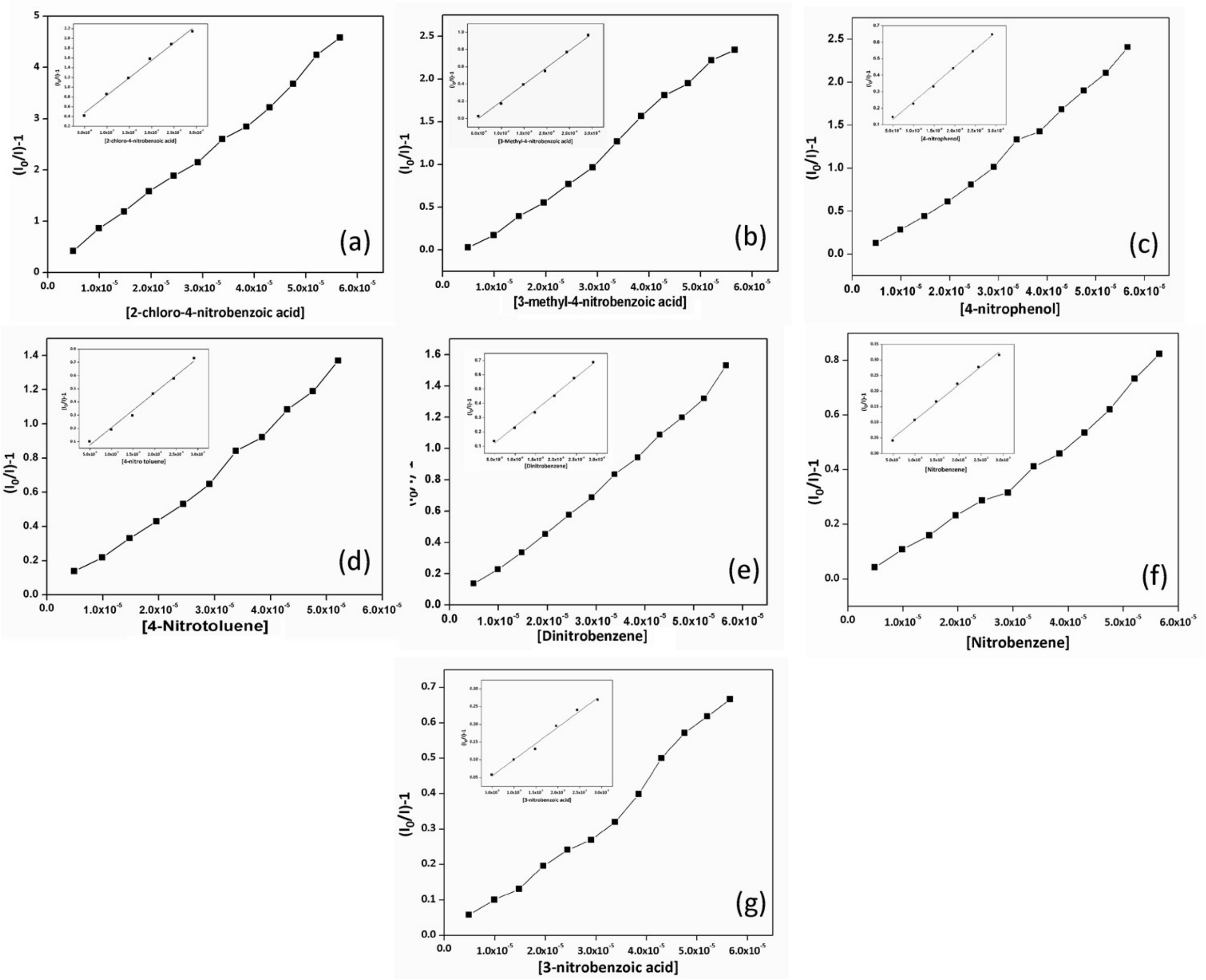

Fig. S22: Stern–Volmer plot of complex **2** with 2-chloro-4-nitrobenzoic acid (a), 3-methyl-4-nitrobenzoic acid (b), 4-nitrophenol (c), 4-nitrotoluene (d), dinitrobenzene (e), nitrobenzene (f), 3-nitrobenzoic acid (g) in DMF.

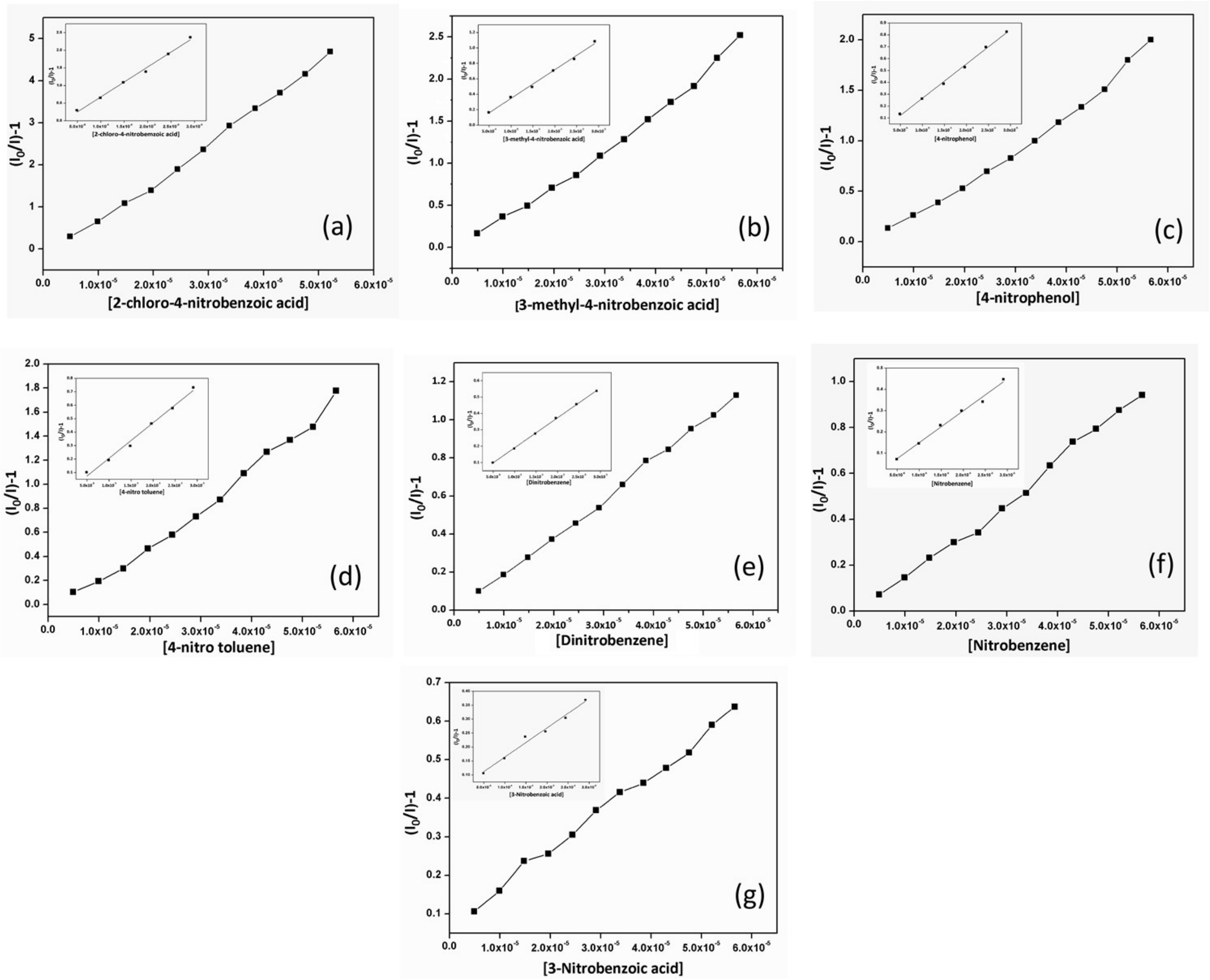

Fig. S23: Stern–Volmer plot of complex **3** with 2-chloro-4-nitrobenzoic acid (a), 3-methyl-4-nitrobenzoic acid (b), 4-nitrophenol (c), 4-nitrotoluene (d), dinitrobenzene (e), nitrobenzene (f), 3-nitrobenzoic acid (g) in DMF.

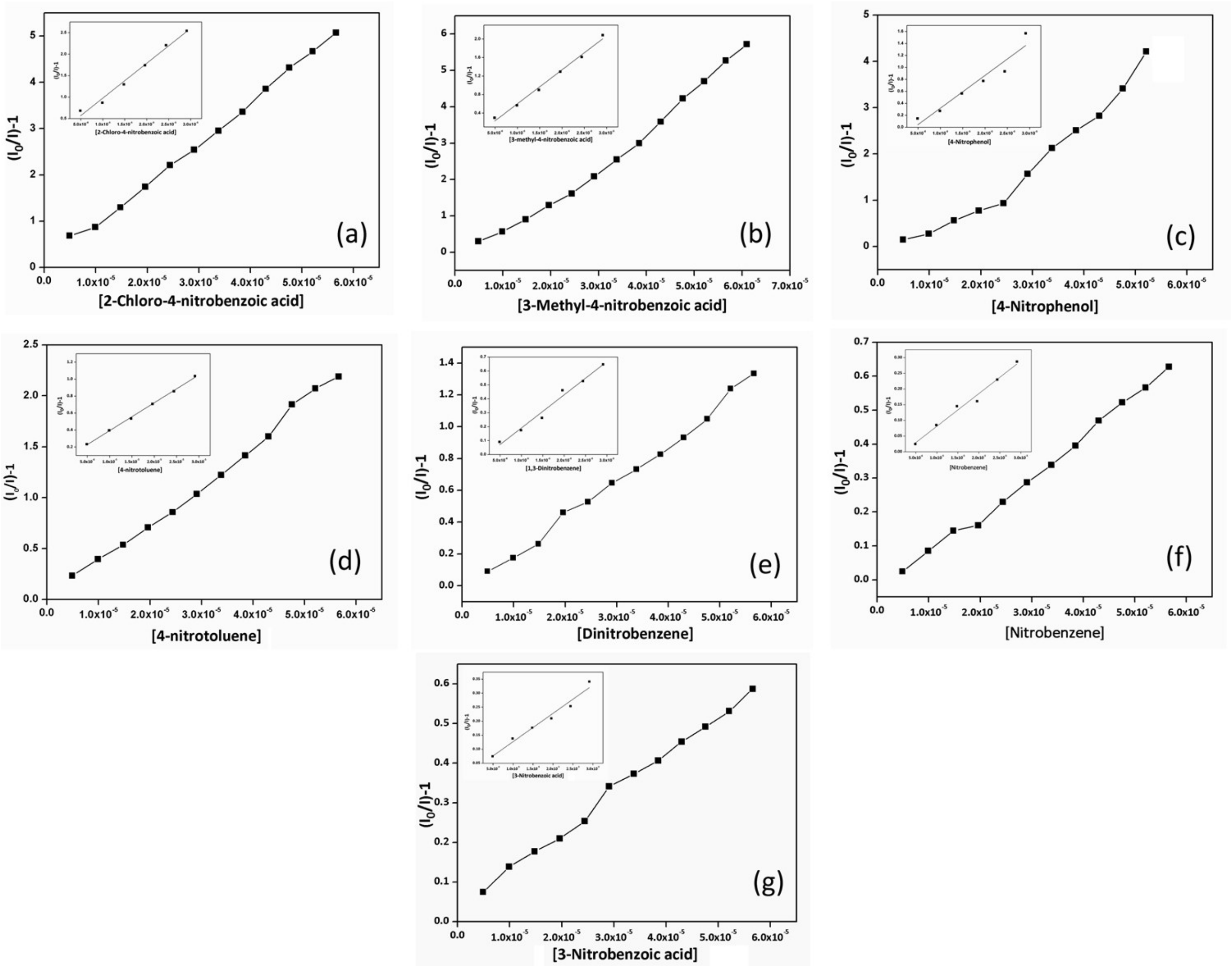

Fig. S24: Stern–Volmer plot of complex **4** with 2-chloro-4-nitrobenzoic acid (a), 3-methyl-4-nitrobenzoic acid (b), 4-nitrophenol (c), 4-nitrotoluene (d), dinitrobenzene (e), nitrobenzene (f), 3-nitrobenzoic acid (g) in DMF.

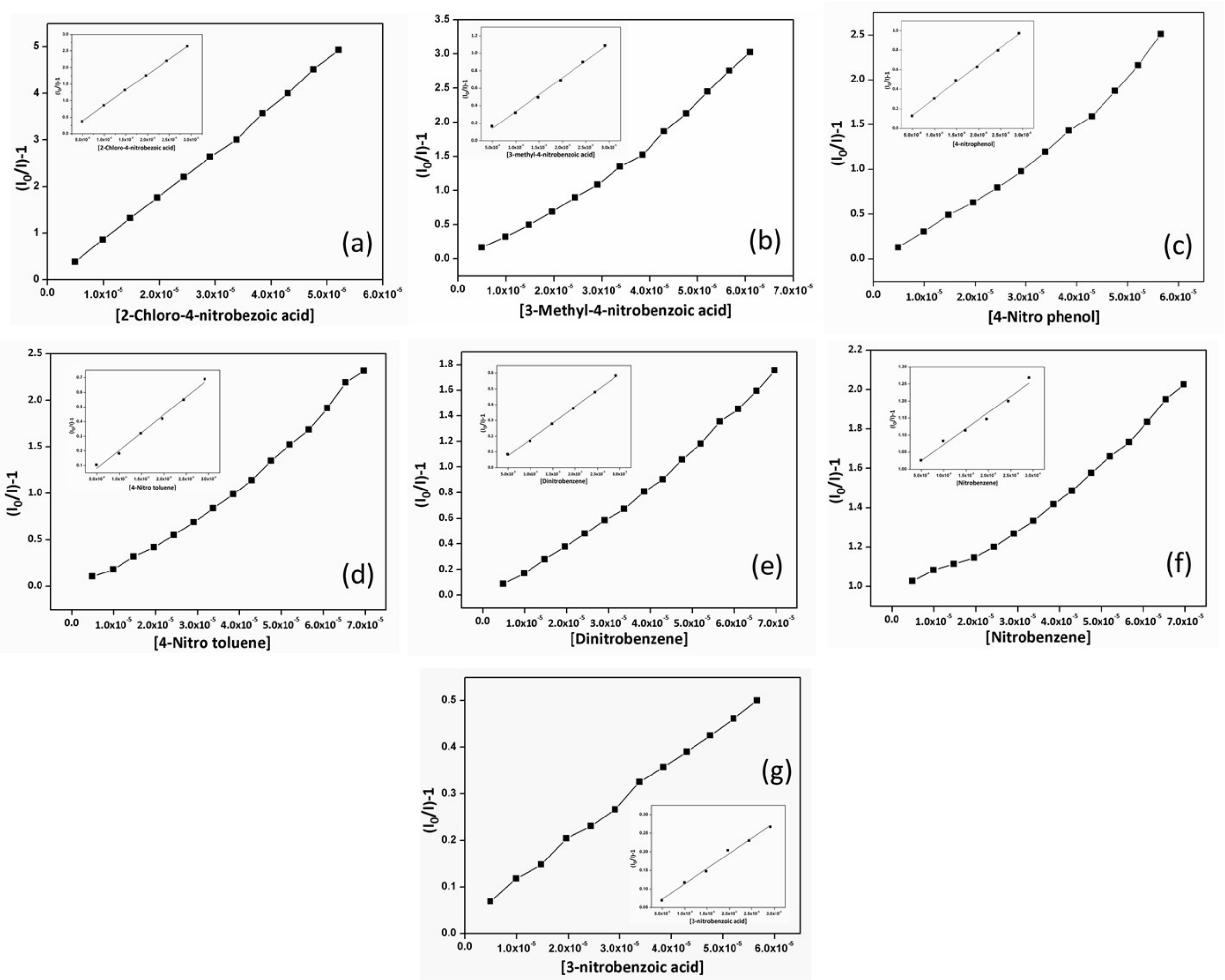

Fig. S25: Stern–Volmer plot of complex **5** with 2-chloro-4-nitrobenzoic acid (a), 3-methyl-4-nitrobenzoic acid (b), 4-nitrophenol (c), 4-nitrotoluene (d), dinitrobenzene (e), nitrobenzene (f), 3-nitrobenzoic acid (g) in DMF.

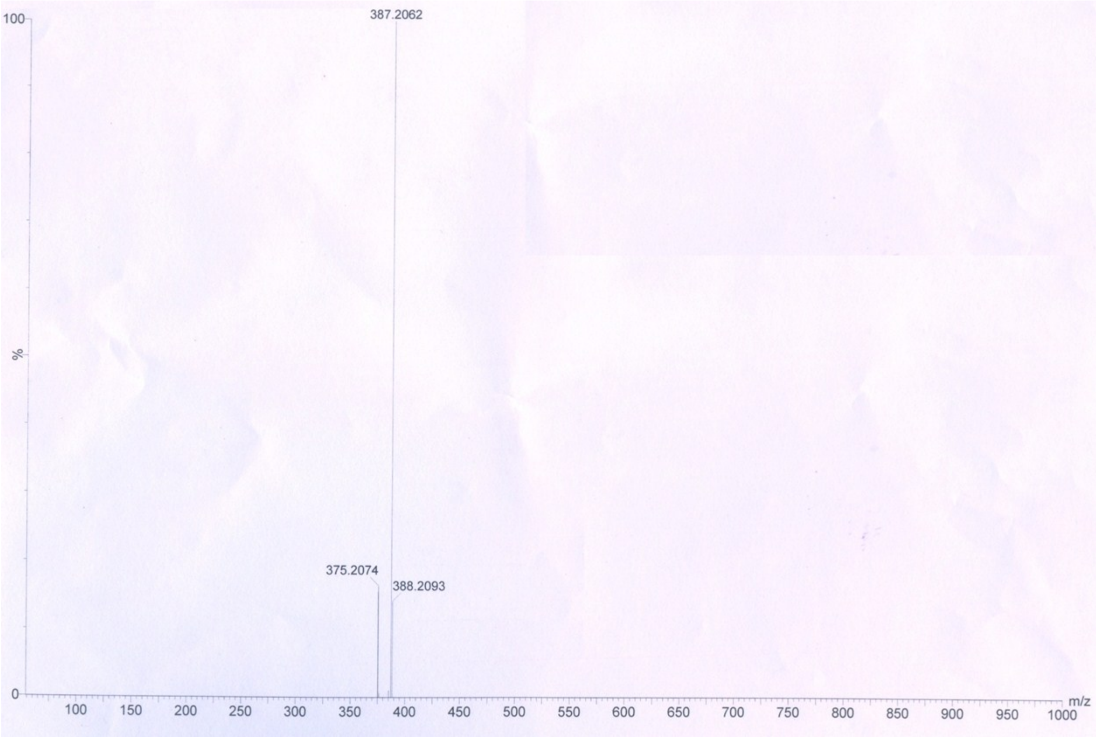

Fig. S26(a). Mass spectrum of complex **3** with 2-chloro-4-nitrobenzoic acid in DMF (Full scale).

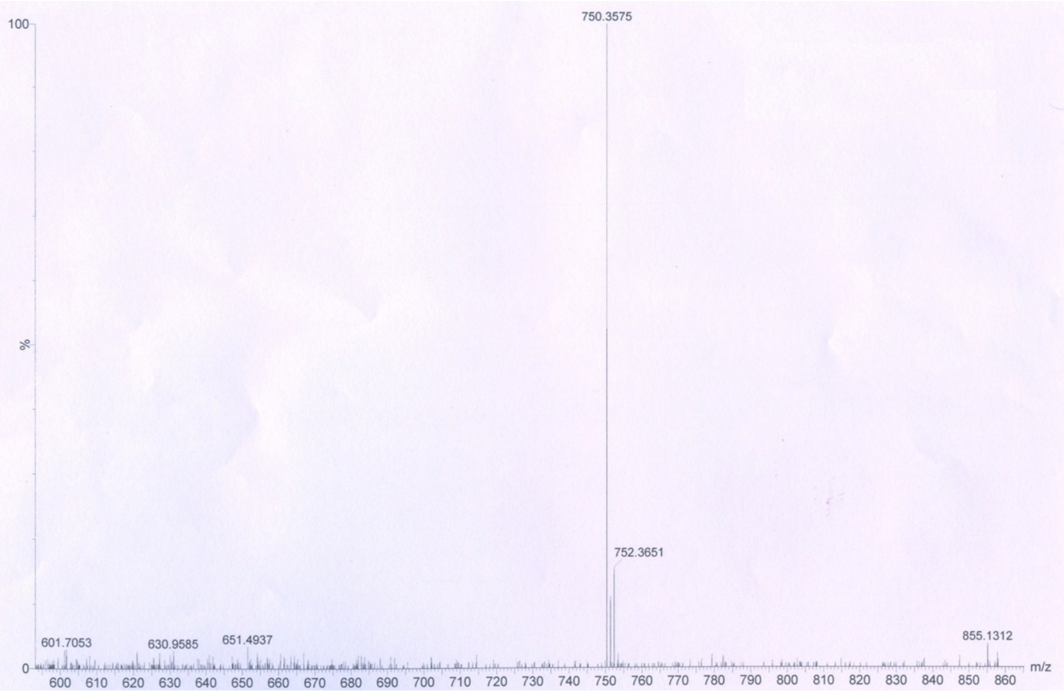

Fig. S26(a). Mass spectrum of complex **3** with 2-chloro-4-nitrobenzoic acid in DMF (Selected range 600-860).

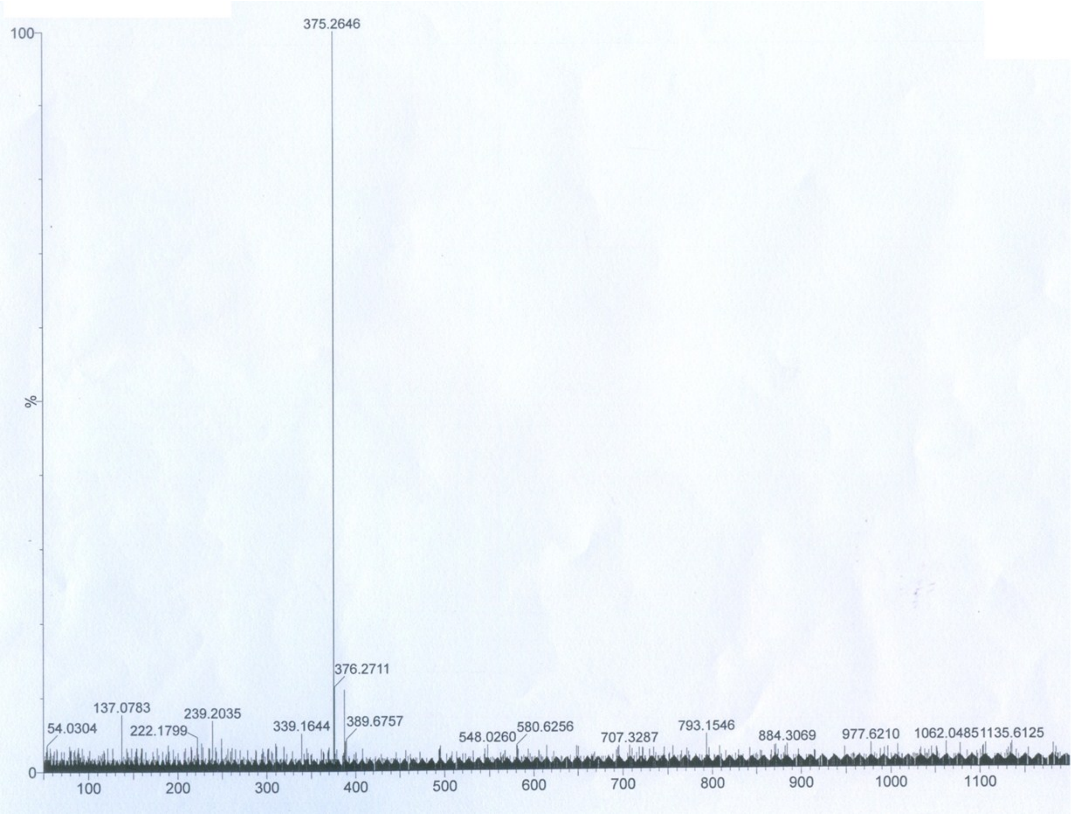

Fig. S27. Mass spectrum of complex **3** with 4-nitrophenol in DMF (Full scale).

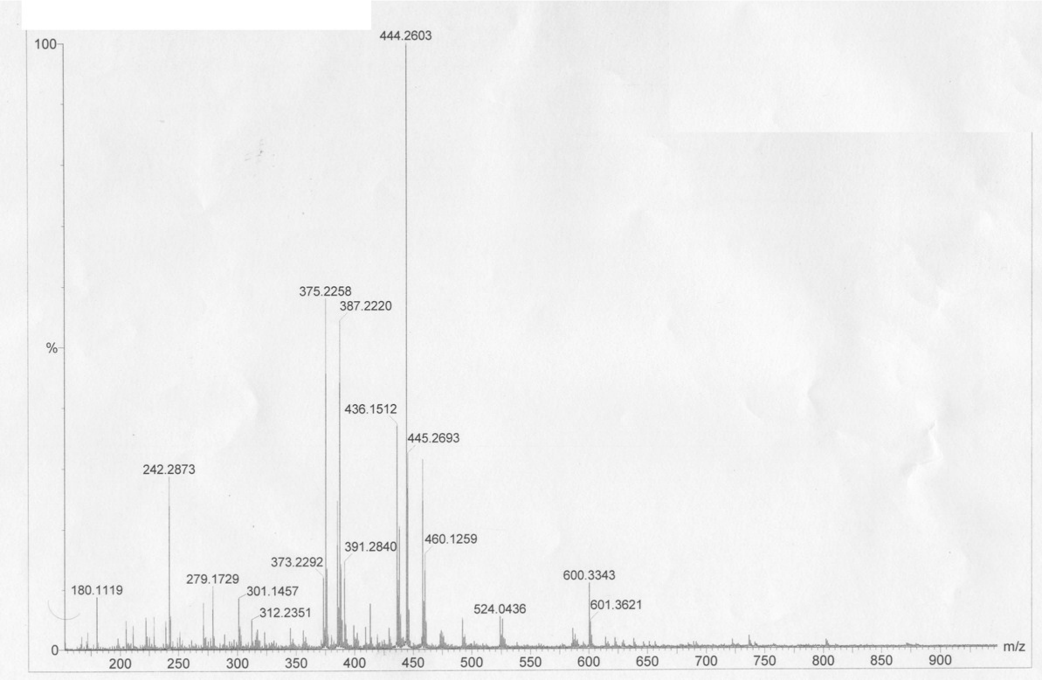

Fig. S28. Mass spectrum of complex **3** with 4-nitrotoluene in DMF (Full scale).

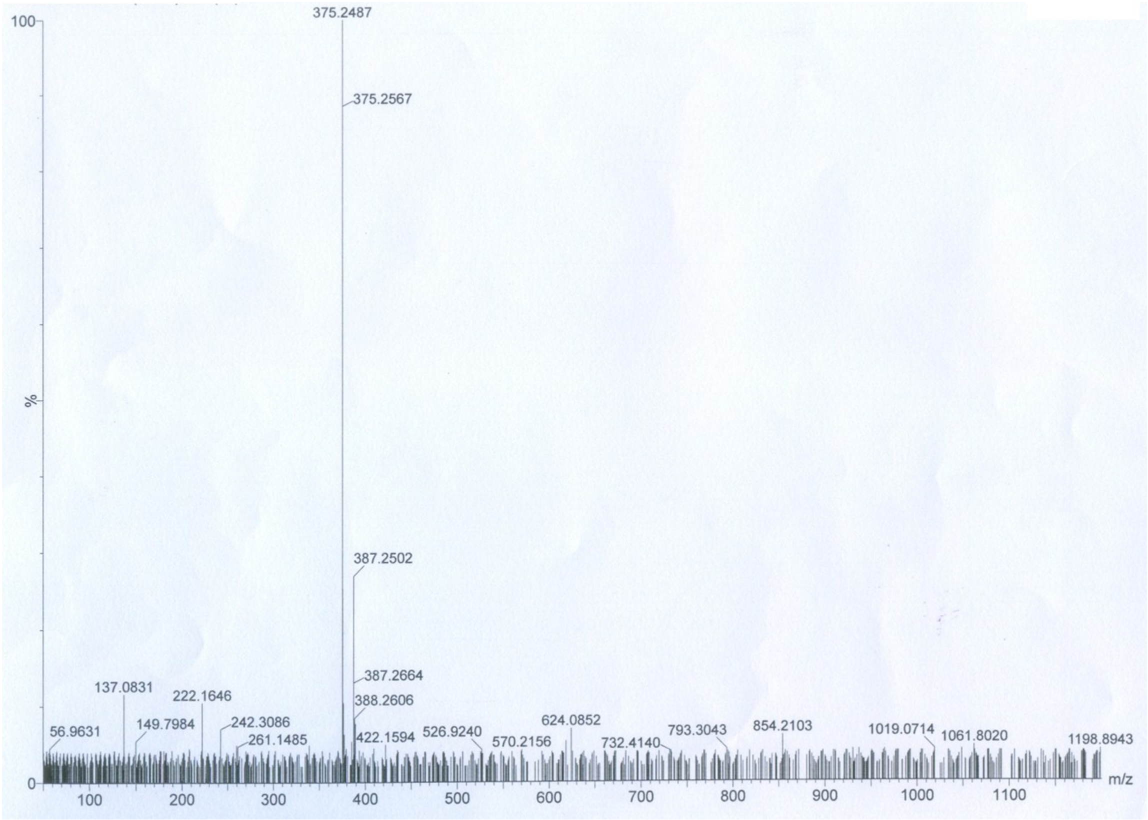

Fig. S29. Mass spectrum of complex **3** with dinitrobenzene in DMF (Full scale).

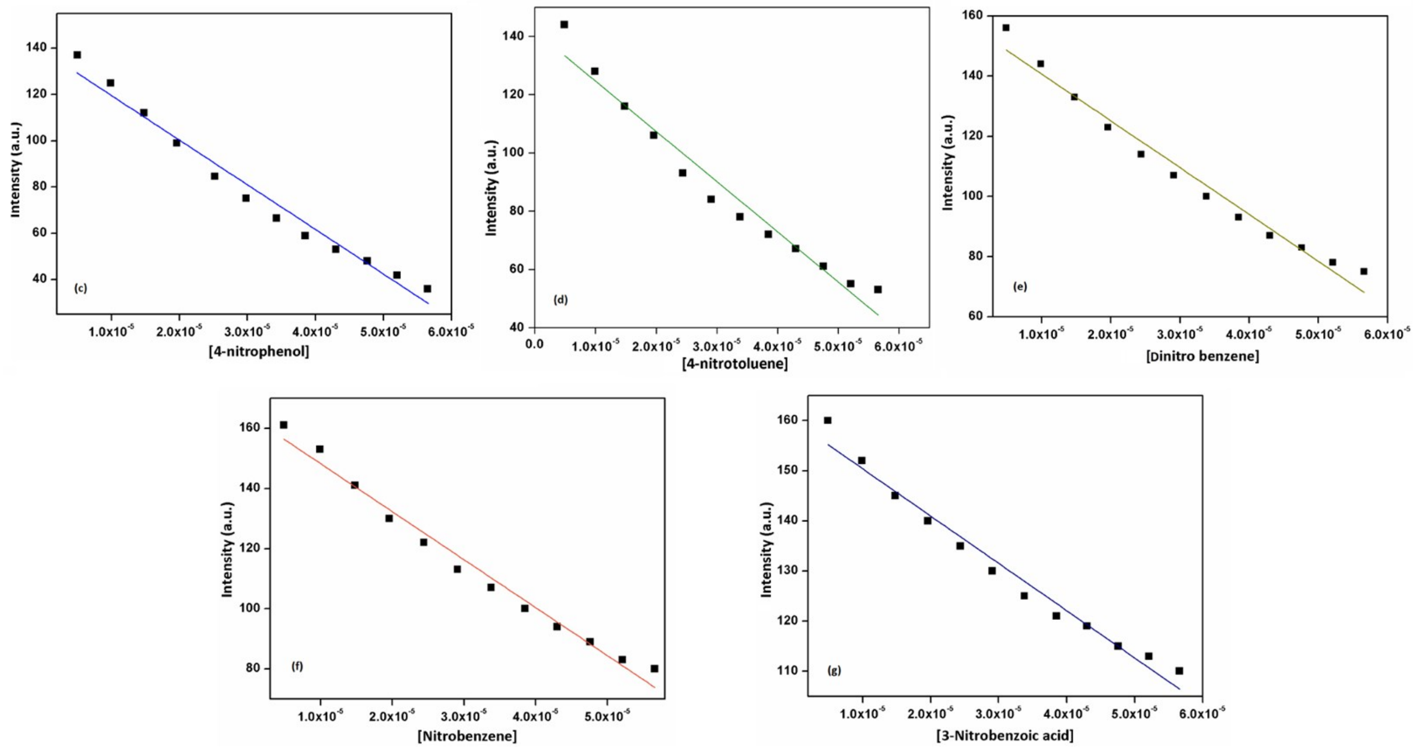

Fig. S30: Plot of limit of detection for complex **1** towards 4-nitrophenol (a), 4-nitrotoluene (b), dinitrobenzene (c), nitrobenzene (d), 3-nitrobenzoic acid (e) in DMF.

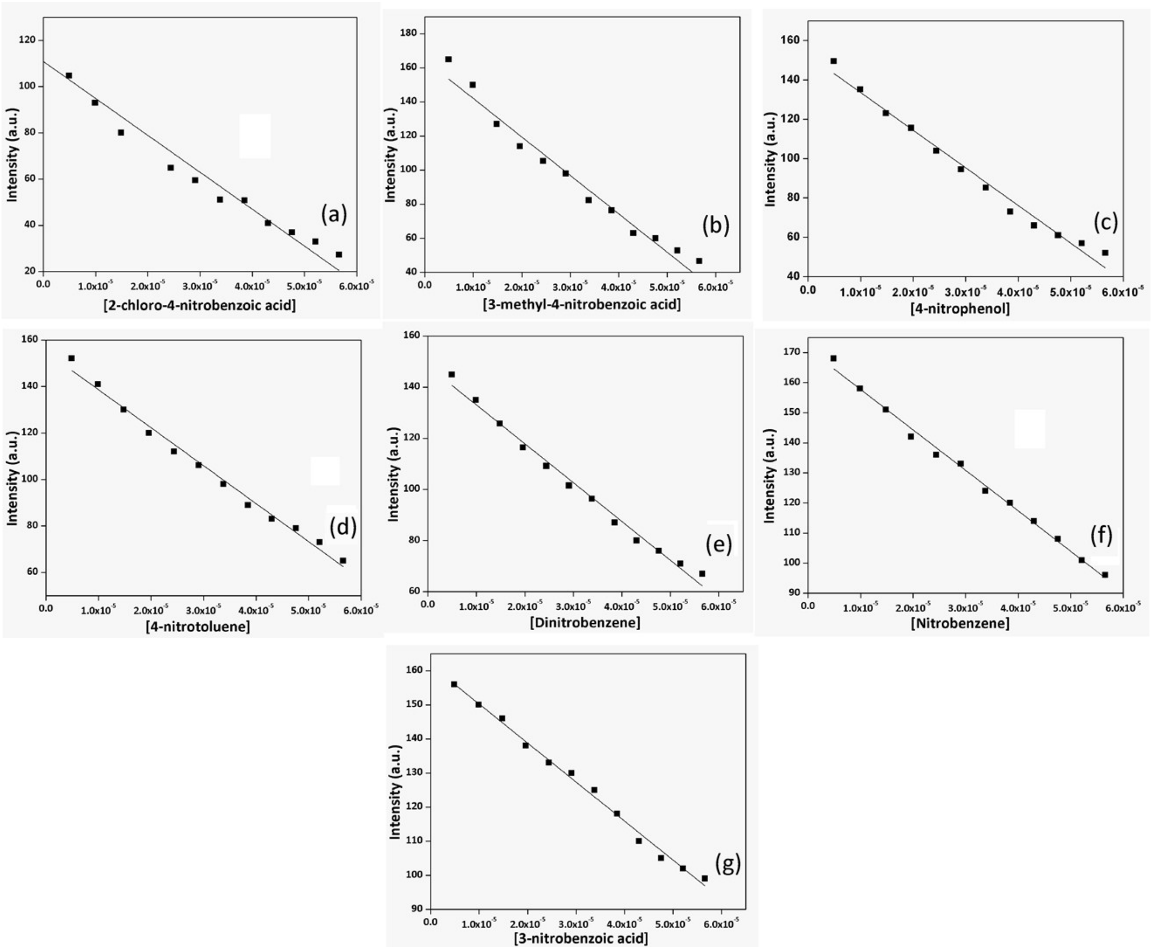

Fig. S31: Plot of limit of detection for complex **2** towards 2-chloro-4-nitrobenzoic acid (a), 3-methyl-4-nitrobenzoic acid (b), 4-nitrophenol (c), 4-nitrotoluene (d), dinitrobenzene (e), nitrobenzene (f), 3-nitrobenzoic acid (g) in DMF.

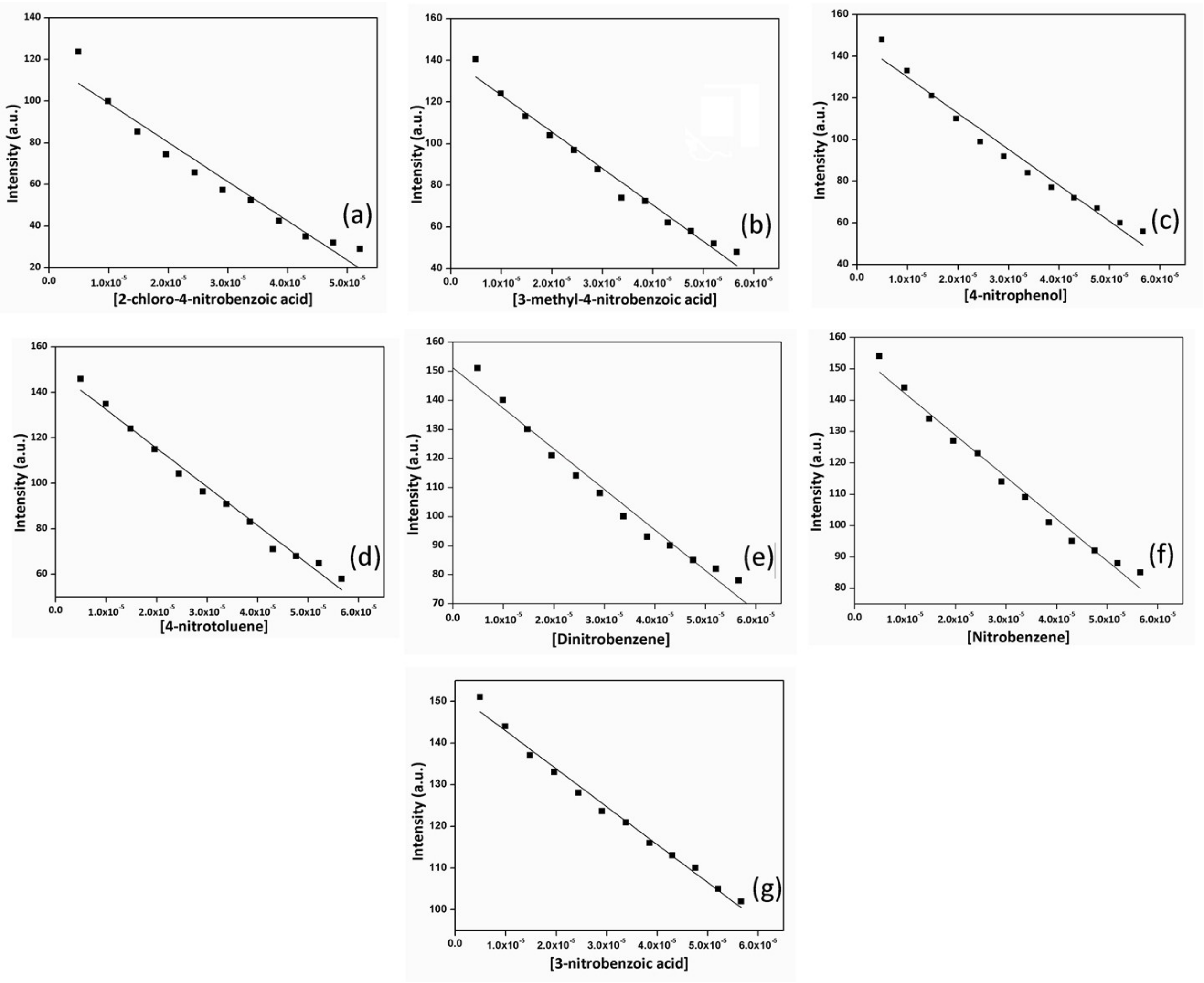

Fig. S32: Plot of limit of detection for complex **3** towards 2-chloro-4-nitrobenzoic acid (a), 3-methyl-4-nitrobenzoic acid (b), 4-nitrophenol (c), 4-nitrotoluene (d), dinitrobenzene (e), nitrobenzene (f), 3-nitrobenzoic acid (g) in DMF.

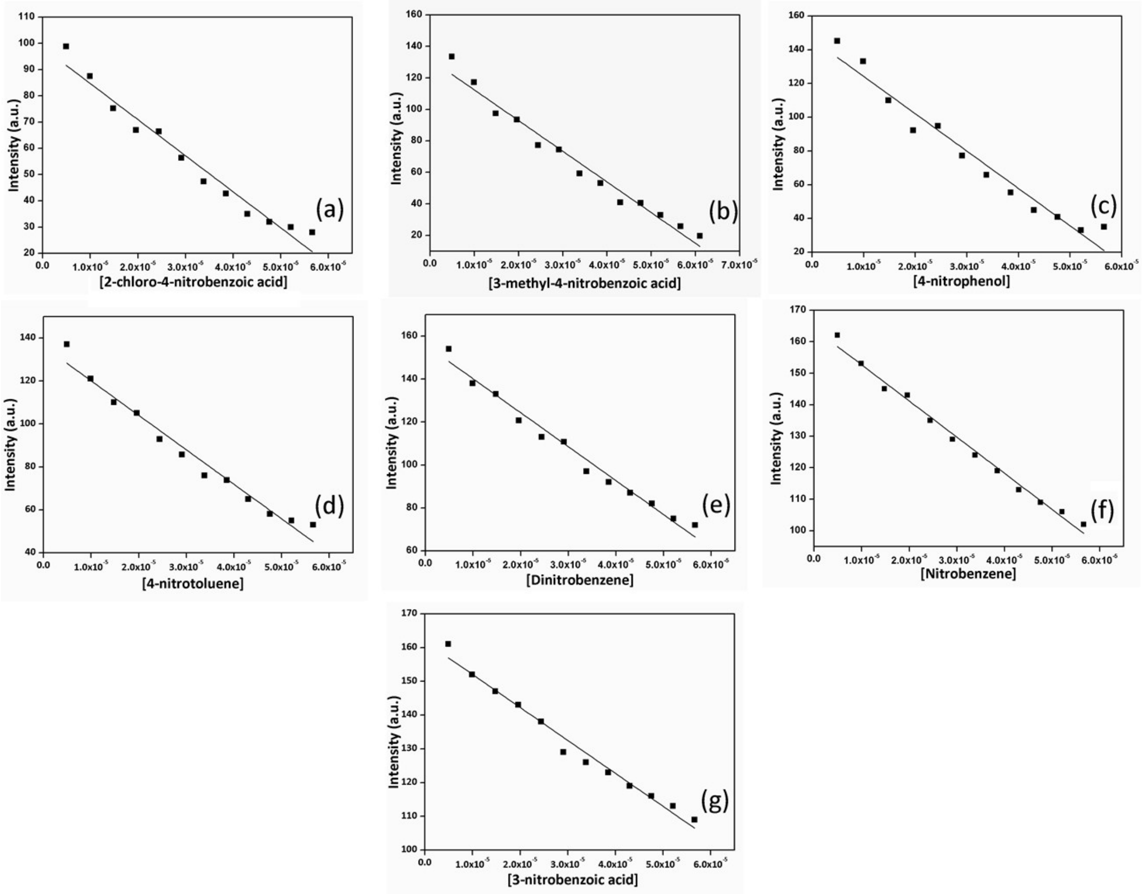

Fig. S33: Plot of limit of detection for complex **4** towards 2-chloro-4-nitrobenzoic acid (a), 3-methyl-4-nitrobenzoic acid (b), 4-nitrophenol (c), 4-nitrotoluene (d), dinitrobenzene (e), nitrobenzene (f), 3-nitrobenzoic acid (g) in DMF.

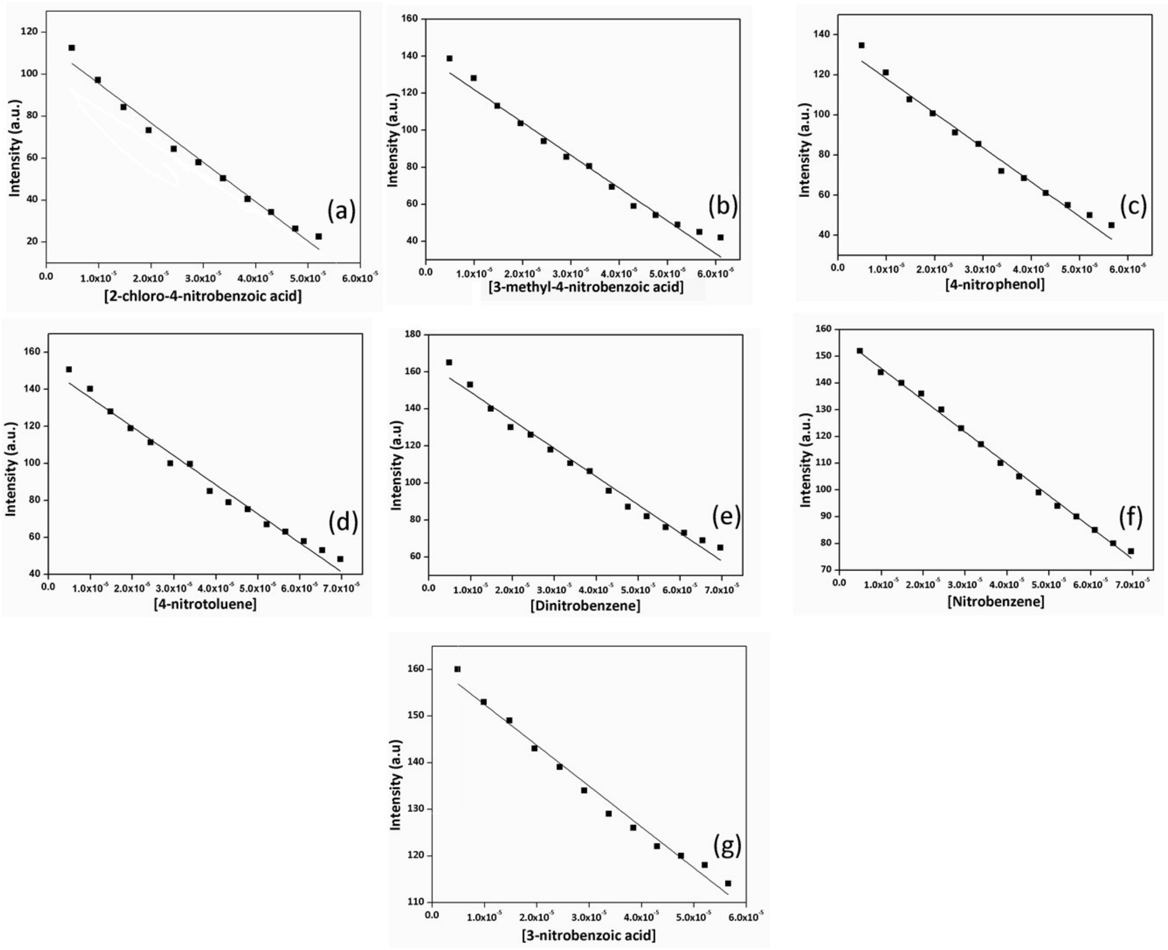

Fig. S34: Plot of limit of detection for complex **5** towards 2-chloro-4-nitrobenzoic acid (a), 3-methyl-4-nitrobenzoic acid (b), 4-nitrophenol (c), 4-nitrotoluene (d), dinitrobenzene (e), nitrobenzene (f), 3-nitrobenzoic acid (g) in DMF.

References

1 (a) G. M. Sheldrick, *ActaCrystallogr., Sect.*, 2008, **A64**, 112-122; (b) G. M. Sheldrick, *Actacrystallogr., Sect., Structural chemistry,* 2015, **C71**, 3-8.

2 G. M. Sheldrick, SADABS, V2014/5, Software for Empirical Absorption Correction, University of Göttingen, Institute fur AnorganischeChemiederUniversitat, Gottingen, Germany, 1999–2003.

3 (a) M. A. Spackman and P. G. Byrom, *Chem. Phys. Lett.*, 1997, **267**, 215-220; (b) J. J. McKinnon, M. A. Spackman and A. S. Mitchell, *Acta Cryst. B*, 2004, **60**, 627-668.

4 J. J. McKinnon, D. Jayatilaka and M. A. Spackman, *Chem Commun.*, 2007, 3814-3816.

5 (a) J. J. Koenderink and A. J. Van Doorn, *Image and Vision Computing*, 1992, **10**, 557; (b) J. J. McKinnon, M. A. Spackman and A. S. Mitchell, *Acta Cryst. B*, 2004, **60**, 627-668; (c) M. A. Spackman and D. Jayatilaka, *CrystEngComm*, 2009, **11**, 19-32.

6 A. L. Rohl, M. Moret, W. Kaminsky, K. Claborn, J. J. McKinnon and B. Kahr, *Cryst. Growth Des.,* 2008, **8**, 4517-4525.

7 (a) S. Jana, P. Bhowmik, M. Das, P. P. Jana, K. Harms and S. Chattopadhyay, *Polyhedron*, 2012, **37** 21-26, (b) P. Bhowmik, H. P. Nayek, M. Corbella, N. A. Alcalde and S. Chattopadhyay, *Dalton Trans*., 2011, **40**, 7916-7926; (c) A. Bhattacharyya, S. Roy, J. Chakraborty and S. Chattopadhyay, *Polyhedron* 2016, **112**, 109-117.

8 (a) M. Das, K. Harms and S. Chattopadhyay, *Dalton Trans*., 2014, **43**, 5643-5647; (b) P. Bhowmik, S. Jana and S. Chattopadhyay, *Polyhedron*, 2012, **44**, 11-17.

9 (a) P. Bhowmik, S. Chatterjee and S. Chattopadhyay, *Polyhedron*, 2013, **63**, 214-221; (b) S. Roy, M. G. B. Drew, A. Bauzá and A. Frontera, *CrystEngComm*, 2018, **20**, 1679-1689.

10 (a) P. K. Bhaumik, S. Roy, K. Harms and S. Chattopadhyay, *Polyhedron*, 2014, **81**, 168-179; (b) S. Roy, P. K. Bhaumik, K. Harms and S. Chattopadhyay, *Inorg. Chim. Acta*, 2015, **427**, 155-161; (c) A. Bhattacharyya, S. Sen, K. Harms and S. Chattopadhyay, *Polyhedron*, 2015, **88**, 156-163; (d) M. Amirnasr, A. H. Mahmoudkhani, A. Gorji, S. Dehghanpour, H. R. Bijanzadeh, *Polyhedron,* 2002, **21**, 2733-2742.